

Noname manuscript No.
(will be inserted by the editor)

On efficiency of nonmonotone Armijo-type line searches

Masoud Ahookhosh · Susan Ghaderi

Abstract Monotonicity and nonmonotonicity play a key role in studying the global convergence and the efficiency of iterative schemes employed in the field of nonlinear optimization, where globally convergent and computationally efficient schemes are explored. This paper addresses some features of descent schemes and the motivation behind nonmonotone strategies and investigates the efficiency of an Armijo-type line search equipped with some popular nonmonotone terms. More specifically, we propose two novel nonmonotone terms, combine them into Armijo's rule and establish the global convergence of sequences generated by these schemes. Furthermore, we report extensive numerical results and comparisons indicating the performance of the nonmonotone Armijo-type line searches using the most popular search directions for solving unconstrained optimization problems. Finally, we exploit the considered nonmonotone schemes to solve an important inverse problem arising in signal and image processing.

Keywords Unconstrained optimization · Armijo-type line search · Nonmonotone strategy · Global convergence · Computational efficiency · First- and second-order black-box information

Mathematics Subject Classification (2000) 90C30 · 65K05

1 Introduction

In this paper, we shall be concerned with some iterative schemes for solving the unconstrained minimization problem

$$\begin{aligned} & \text{minimize} && f(x) \\ & \text{subject to} && x \in \mathbb{R}^n. \end{aligned} \tag{1}$$

where $f : \mathbb{R}^n \rightarrow \mathbb{R}$ is a real-valued nonlinear function, which is bounded and continuously-differentiable. We suppose that first- or second-order black-box information of f is available.

Motivation & history. Over the last five decades many iterative schemes for locally solving (1) have been established according to the availability of information of the objective function f . Indeed, the conventional approaches are **descent** methods, also called **monotone** methods, generating a sequence of iterations such that the corresponding sequence of function values is monotonically decreasing, see [24, 38]. There exists a variety of descent methods that are classified in accordance with required information of the objective function in terms of computing function values and derivatives. More precisely, the availability of first- and second-order black-box information leads to two prominent classes so-called **first-** and **second-order** methods, where first-order methods only need function and gradient evaluations, and second-order methods require function and gradient and Hessian evaluations, see [35].

In general, descent methods determine a descent direction d_k , specify a step-size $\alpha_k \in (0, 1]$ by an inexact line search such as Armijo, Wolfe or Goldstein backtracking schemes, generate a new iteration

M. Ahookhosh
Faculty of Mathematics, University of Vienna, Oskar-Morgenstern-Platz 1, 1090 Vienna, Austria
E-mail: masoud.ahookhosh@univie.ac.at

S. Ghaderi
Department of Mathematics, Faculty of Science, Razi University, Kermanshah, Iran
E-mail: susan.ghaderi23@gmail.com

by setting $x_{k+1} = x_k + \alpha_k d_k$, and repeat this scheme until a stopping criterion holds. The key features of these methods is characterized by choosing an appropriate inexact line search guaranteeing that

- the sequence of function values is monotonically decreasing, i.e., $f_{k+1} \leq f_k$ where $f_k = f(x_k)$;
- the sequence $\{x_k\}$ is convergent globally meaning that the method is convergent for an arbitrary initial point x_0 , especially when x_0 is far away from the minimizer.

The first property seems natural due to the aim of minimizing the objective function, and the second feature makes the method independent on the initial point x_0 . In particular, Armijo's line search satisfies

$$f(x_k + \alpha_k d_k) \leq f_k + \sigma \alpha_k g_k^T d_k, \quad (2)$$

where $g_k = \nabla f(x_k)$, $\sigma \in (0, \frac{1}{2})$, and α_k is the largest $\alpha \in \{s, \rho s, \dots\}$ with $s > 0$ and $\rho \in (0, 1)$ such that (2) holds, see [9]. Since the direction d_k is descent, i.e. $g_k^T d_k < 0$, function values satisfy the condition $f_{k+1} \leq f_k$ imposing the monotonicity to the sequence $\{f_k\}$ generated by this scheme. Moreover, it is globally convergent, see for example [38]. A version of descent algorithms using Armijo's rule is outlined in the following:

Algorithm 1: DATA (descent Armijo-type algorithm)

Input: $x_0 \in \mathbb{R}^n$, $\rho \in (0, 1)$, $\sigma \in (0, \frac{1}{2})$, $s \in (0, 1]$, $\epsilon > 0$;
Output: x_b ; f_b ;
begin
 $k \leftarrow 0$; compute f_0 ;
 while $\|g_k\| \geq \epsilon$ **do**
 generate a descent the direction d_k ;
 $\alpha \leftarrow s$; $\hat{x}_k \leftarrow x_k + \alpha d_k$;
 while $f(\hat{x}_k) > f_k + \sigma \alpha g_k^T d_k$ **do**
 $\alpha \leftarrow \rho \alpha$; $\hat{x}_k \leftarrow x_k + \alpha d_k$;
 end
 $x_{k+1} \leftarrow \hat{x}_k$; $k \leftarrow k + 1$;
 end
 $x_b \leftarrow x_k$, $f_b \leftarrow f_k$;
 end

Despite the advantages considered for imposing monotonicity to the sequence of function values, it causes some difficulties. We here mention two important cases:

- The algorithm losses its efficiency if an iteration is trapped close to the bottom of a curved narrow valley of the objective function, where the monotonicity enforces iterations to follow the valley's floor causing very short steps or even undesired zigzagging, see for example [25, 43]. In the sequel, we will verify this fact in Examples 1 and 2;
- The Armijo-type backtracking line search can break down for small step-sizes because of the condition $f(x_k + \alpha d_k) \simeq f_k$ and rounding errors. In such a situation, the step x_k may still be far from the minimizer of f , however, the Armijo condition cannot be verified because the function values required to be compared are indistinguishable in the floating-point arithmetic, i.e.,

$$0 \simeq f(x_k + \alpha d_k) - f_k > \sigma \alpha g_k^T d_k$$

since $g_k^T d_k < 0$ and $\sigma, \alpha > 0$, see [15].

These disadvantages of descent methods have inspired many researchers to work on some improvements to avoid such drawbacks. In the remainder of this section, some of these developments will be reviewed.

According to the availability of first- or second-order information of f , the direction d_k can be determined in various ways imposing different convergence theories and computational results, [24, 38, 35]. On the one hand, first-order methods only need function values and gradients leading to low memory requirement making them appropriate to solve large-scale problems. On the other hand, if second-order information is available, the classical method for solving (1) is **Newton**'s method producing an excellent local convergence. More specifically, Newton's method minimizes the quadratic approximation of the objective function, where the corresponding direction is derived by solving the linear system

$$H_k d_k = -g_k, \quad (3)$$

in which H_k is Hessian of f evaluated at the current iterate x_k . Indeed, if Hessian is positive definite and the dimension of the problem is not very large, Newton's method is possibly the most successful descent method for minimizing a twice continuously-differentiable function. The derivation of Newton's method implies that it converges to the stationary point of a quadratic function in one iteration. However, for general functions, it usually exhibits a quadratic convergence rate near the solution, however, there is no reason to expect that Newton's method behaves well if x_0 is chosen far away from the optimizer x^* , see [40]. This implies that Newton's method can be enhanced to obtain the global convergence, which is the convergence to a stationary point from an arbitrary starting point x_0 that may be far away from it. A globally convergent modification of Newton's method is called **damped Newton**'s method exploiting Newton's direction (3) and a line search similar to that discussed in Algorithm 1.

The sequence produced by Algorithm 1 converges to an ϵ -solution x^* satisfying $\|\nabla f(x^*)\| < \epsilon$, which is by no means sufficient to guarantee that x^* is a local minimizer. Indeed, it can converge to a local maximizer or a saddle point. Furthermore, if the iterate x_k is trapped in the bottom of a deep narrow valley, it generates very short steps to keep the monotonicity resulting to a very slow convergence. This fact clearly means that employing a monotone line search to ensure the global convergence can ruin the excellent local convergence of Newton's method. We verify this fact in the next example.

Example 1 Consider two-dimensional Rosenbrock's function

$$f(x) = (x_2 - x_1^2)^2 + (1 - x_1)^2.$$

We solve the problem (1) by Newton's method and damped Newton's method with the initial point $x_0 = (-\frac{1}{10}, \frac{1}{10})$. It is clear that $(1, 1)$ is the optimizer. The implementation indicates that damped Newton's method needs 15 iterations and 17 function evaluations while Newton's method needs only 7 iterations and 8 function evaluations. To study the result more precisely, we depict the contour plot of the objective function and iterations attained by these two algorithms in Figure 1. Subfigure (a) of Figure 1 shows that iterations of damped Newton's method follow the bottom of the valley in contrast to those for Newton's method that can go up and down to reach the ϵ -solution with the accuracy parameter $\epsilon = 10^{-5}$. We see that Newton's method attains larger step-sizes compared with those of damped Newton's method. Subfigure (b) of Figure 1 illustrates function values versus iterations for both algorithms showing that the related function values of damped Newton's method decreases monotonically while it is fluctuated nonmonotonically for Newton's method.

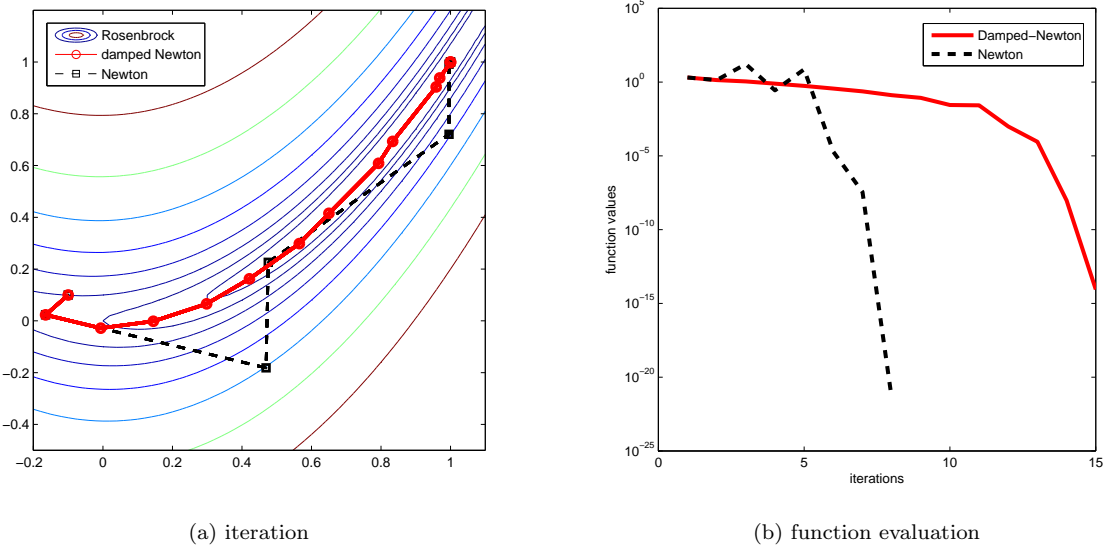


Fig. 1: A comparison between Newton and damped Newton methods: (a) the contour plot of Rosenbrock's function and iterations of Newton and damped Newton methods; (b) the function values vs. iterations.

Thanks to the increasing interest in using nonlinear optimization during the few past decades and to avoid the above-mentioned drawbacks of monotone schemes, many researchers have conducted lots of investigations on developing methods guaranteeing the global convergence and preserving the local convergence rate of descent methods at the same time. The pioneering work dating back to 1986 proposed by GRIPPO et al. in [25] introducing a variant of Armijo's rule using the term $f_{l(k)}$ in place of f_k in (2) defined by

$$f_{l(k)} = \max_{0 \leq j \leq m(k)} \{f_{k-j}\}, \quad k = 0, 1, 2, \dots, \quad (4)$$

where $m(0) = 0$ and $0 \leq m(k) \leq \min\{m(k-1) + 1, N\}$ with a positive constant $N \in \mathbb{N}$. The fact that $f_{l(k)} \geq f_k$ along with the convergence theory presented in [25] reveal the following properties of the modified Armijo-type line search :

- The sequence $\{x_k\}$ generated by the new scheme is still globally convergent to first-order stationary points of f ;
- The function value at the new point $x_{k+1} = x_k + \alpha_k d_k$ can be greater than f_k , so the sequence of function values $\{f_k\}$ is not monotonically decreasing, similar to the natural behaviour of the pure Newton method. However, the subsequence $\{f_{l(k)}\}$ of $\{f_k\}$ is still monotonically decreasing, see [25].
- The right hand side of the new Armijo-type line search is greater than original Armijo's rule implying that the new method can take bigger step-sizes compared to descent methods using original Armijo's rule (2);
- In original Armijo's rule, if no step-size can be found to satisfy (2), the algorithm usually stops by rounding errors preventing further progress. Since $f_{l(k)} \geq f_k$, it is much less possible that rounding errors break down the new nonmonotone line search.

Since the new line search is not imposing the monotonicity to the sequence of function values, it is called **nonmonotone**. The corresponding numerical results for the nonmonotone Armijo's rule reported in [25, 43] are totally interesting. We verify the efficiency of this scheme in the subsequent example for the gradient descent direction and the Barzilai-Borwein direction described in Section 3.3.

Example 2 We now consider Rosenbrock's function described in Example 1 and solve (1) by the gradient descent method and a version of Barzilai-Borwein method using the nonmonotone line search of GRIPPO et al. in [25]. In our implementation, gradient descent and Barzilai-Borwein methods require 11987 and 45 iterations and 118449 and 53 function evaluations, respectively. Subfigure (a) of Figure 2 implies that iterations of the gradient descent method zigzag at the bottom of the valley while the iterations of the Barzilai-Borwein method go up and down from both sides of the valley. Subfigure (b) implies that the Barzilai-Borwein method is substantially superior to the gradient descent method and the corresponding sequence of function values behaves nonmonotonically in contrast to that for the gradient descent method.

Later the nonmonotone term (4) was used in a more sophisticated algorithm by GRIPPO et al. in [27], and they also proposed a nonmonotone truncated Newton method in [26]. TOINT in [43] conducted extensive numerical results and proposed a new nonmonotone term. For more references, see also [14, 16, 17, 19, 41]. In 2004, some disadvantages of the nonmonotone term (4) were discovered by ZHANG and HAGER in [45], and to avoid them the following nonmonotone term was proposed

$$C_k = \begin{cases} f_k & \text{if } k = 0; \\ (\eta_{k-1} Q_{k-1} C_{k-1} + f_k) / Q_k & \text{if } k \geq 1, \end{cases} \quad Q_k = \begin{cases} 1 & \text{if } k = 0; \\ \eta_{k-1} Q_{k-1} + 1 & \text{if } k \geq 1, \end{cases} \quad (5)$$

where $\eta_{k-1} \in [\eta_{min}, \eta_{max}]$ with $\eta_{min} \in [0, 1]$ and $\eta_{max} \in [\eta_{min}, 1]$. It is easy to see that this term is a weighted combination of all accepted function values of their scheme. Their algorithm combines the new term (5) into a Wolfe-type line search producing favourable results. Recently, another term constructed based of a convex combination of all former successful function values investigated by MO et al. in [32] and AHOOKHOSH et al. in [4], where it is defined by

$$D_k = \begin{cases} f_0 & \text{if } k = 0; \\ f_k + \eta_{k-1}(D_{k-1} - f_k) & \text{if } k \geq 1, \end{cases} \quad (6)$$

in which $\eta_{k-1} \in [\eta_{min}, \eta_{max}]$ with $\eta_{min} \in [0, 1]$ and $\eta_{max} \in [\eta_{min}, 1]$. Combination of this term by Armijo's rule shows a promising computational behaviour, see [4]. More recently, AMINI et al. in [6] proposed a new nonmonotone term relaxing the max-based term (4) by an adaptive convex combination of $f_{l(k)}$ and f_k , which is defined by

$$R_k = \eta_k f_{l(k)} + (1 - \eta_k) f_k, \quad (7)$$

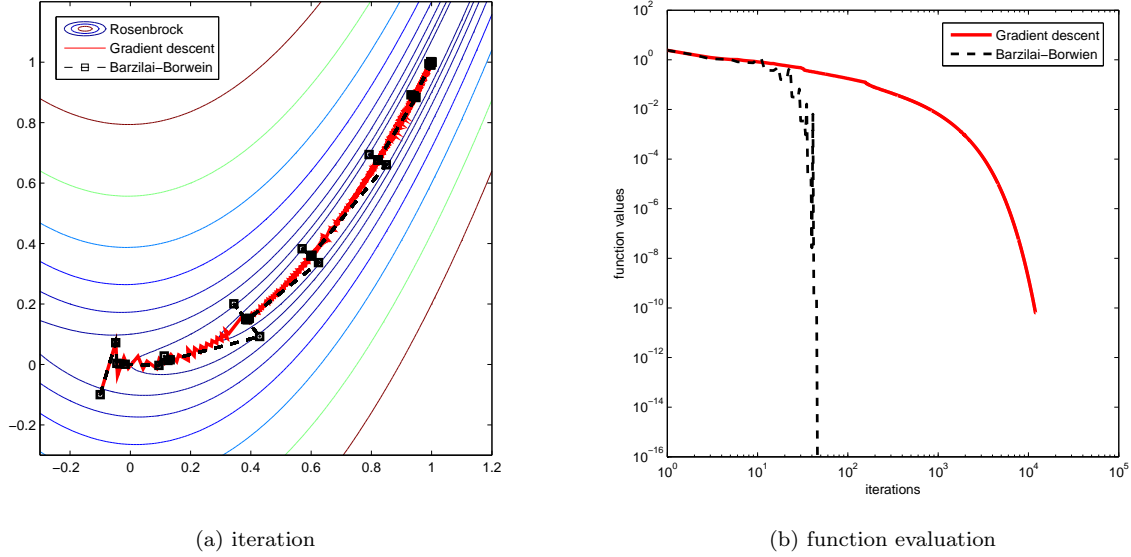


Fig. 2: A comparison between gradient descent and Barzilai-Borwein methods: (a) the contour plot of Rosenbrock's function and iterations of the considered methods; (b) the function values vs. iterations.

in which $\eta_k \in [\eta_{\min}, \eta_{\max}]$ with $\eta_{\min} \in [0, 1]$ and $\eta_{\max} \in [\eta_{\min}, 1]$, see also [2, 5]. This nonmonotone term exploits an adaptive determination of the convexity parameter η_k . Indeed, it uses bigger η_k far from the optimizer and smaller ones close to it. The reported numerical results, which was tested for Brazilai-Borwein, LBFGS and truncated Newton directions, indicate that by using an appropriate sequence $\{\eta_k\}$ the scheme behaves favourably.

An algorithm is considered to be efficient if its computational cost to reach an ε -solution optimizer is at or below some prescribed level of running time and memory usage. In general, the efficiency depend on the way in which the input data is arranged and can be measured by various measures that are generally depend on the size of the input data. In practice, there are some more factors which can affect the efficiency of an algorithm, such as requirements for accuracy and reliability. Since the most computational cost and the related running time of Armijo-type line searches are dependent on the computation of function values and gradients, we here measure the efficiency of an algorithm by counting the number of iterations (N_i), the number of gradient evaluations (N_g), the number of function evaluations (N_f) and some combination of them.

Contribution & organization. This paper addresses some nonmonotone terms and combines them into Armijo's line search (2) for solving the unconstrained problem (1). It is clear that the nonmonotone terms (5) and (6) use all previous function values, however if the initial point of an algorithm is far away from the optimizer, it does not make sense to use initial function values to construct a nonmonotone term that cannot tell us too much about the local behaviour of the objective function. In such a case, we prefer to just use the last N function values to construct the new nonmonotone terms. In particular, we propose two novel nonmonotone terms, where the basic idea is to construct the new nonmonotone terms by a convex combination of the last N successful function values if the current iteration counter k is greater than or equal to a positive integer N . In case $k \leq N$, we exploit either the nonmonotone terms (4) or (6). The global convergence to first-order stationary points as well as convergence rates are established under some suitable conditions. The efficiency of Armijo's rule using state-of-the-art nonmonotone terms involving new ones are evaluated by doing extensive numerical experiments on a set of unconstrained optimization test problems.

The remainder of this paper organized as follows. In Section 2, we derive two novel nonmonotone terms and establish and algorithmic framework along with its convergence analysis. Numerical results on a set of various directions are reported in Section 3. Finally, some conclusions are given in Section 4.

2 New algorithm and its convergence

This section addresses two novel nonmonotone strategies and unifies them with Armijo's rule (2) to achieve efficient schemes for solving the problem (1). As discussed in Section 1, the nonmonotone term of GRIPPO et al. involves some disadvantages, see [4, 6, 45]. One claim is that the term $f_{l(k)}$ is sometimes too much big allowing jump over the optimizer, especially close to the optimizer. Furthermore, the nonmonotone terms (5) and (6) exploit all previous function values that may decrease the effect of more recent function values in these terms. In the remainder of this section, we construct two novel nonmonotone terms using a convex combination of a few past function values.

Let fix the current iteration k and the number $N \in \mathbb{N}$. The main idea is to set up a nonmonotone term determined by a convex combination of the last k successful function values if $k < N$ and by a convex combination of the last N successful function values if $k \geq N$. In the other words, we produce new terms using function values collected in the set

$$\mathcal{F}_k = \begin{cases} \{f_0, f_1, \dots, f_k\} & \text{if } k < N; \\ \{f_{k-N+1}, f_{k-N+2}, \dots, f_k\} & \text{if } k \geq N, \end{cases} \quad (8)$$

which should be updated in each iteration. To this end, motivated by the term (6), we construct a new term \bar{T}_k using the subsequent procedure

$$\begin{cases} \bar{T}_0 = f_0 & \text{if } k = 0; \\ \bar{T}_1 = (1 - \eta_0)f_1 + \eta_0 f_0 & \text{if } k = 1; \\ \bar{T}_2 = (1 - \eta_1)f_2 + \eta_1(1 - \eta_0)f_1 + \eta_1\eta_0 f_0 & \text{if } k = 2; \\ \vdots \quad \vdots & \vdots \\ \bar{T}_{N-1} = (1 - \eta_{N-2})f_{N-1} + \eta_{N-2}(1 - \eta_{N-3})f_{N-2} + \dots + \eta_{N-2} \dots \eta_0 f_0 & \text{if } k = N-1; \\ \bar{T}_N = (1 - \eta_{N-1})f_N + \eta_{N-1}(1 - \eta_{N-2})f_{N-1} + \dots + \eta_{N-1} \dots \eta_0 f_0 & \text{if } k = N; \\ \vdots \quad \vdots & \vdots \\ \bar{T}_k = (1 - \eta_{k-1})f_k + \eta_{k-1}(1 - \eta_{k-2})f_{k-1} + \dots + \eta_{k-1} \dots \eta_{k-N}f_{k-N} & \text{if } k \geq N; \end{cases}$$

where $\eta_i \in [0, 1]$ for $i = 0, 1, \dots, N$ are some weight parameters. Hence the new nonmonotone term is generated by

$$\bar{T}_k := \begin{cases} (1 - \eta_{k-1})f_k + \eta_{k-1}\bar{T}_{k-1} & \text{if } k < N; \\ (1 - \eta_{k-1})f_k + \eta_{k-1}(1 - \eta_{k-2})f_{k-1} + \dots + \eta_{k-1} \dots \eta_{k-N}f_{k-N} & \text{if } k \geq N, \end{cases} \quad (9)$$

where $\bar{T}_0 = f_0$ and $\eta_i \in [0, 1]$ for $i = 0, 1, \dots, k$. To show that \bar{T}_k is a convex combination of the function values collected in the set \mathcal{F}_k , it is enough to show the summation of multipliers are equal to one. For $k \geq N$, the definition for \bar{T}_k implies

$$(1 - \eta_{k-1}) + \eta_{k-1}(1 - \eta_{k-2}) + \dots + \eta_{k-1} \dots \eta_{k-N-1}(1 - \eta_{k-N}) + \eta_{k-1} \dots \eta_{k-N} = 1. \quad (10)$$

For $k < N$, a similar equality shows that a summation of the last k multipliers is equal to one. Therefore, the generated term \bar{T}_k is a convex combination of the elements of \mathcal{F}_k .

The definition of \bar{T}_k clearly implies that the set \mathcal{F}_k should be updated and saved in each iteration. Moreover, $N(N+1)/2$ multiplications are required to compute \bar{T}_k . To avoid saving \mathcal{F}_k and decrease the required number of multiplications, we will derive a recursive formula for (9). From the definition of \bar{T}_k for $k \geq N$, it follows that

$$\begin{aligned} \bar{T}_k - \eta_{k-1}\bar{T}_{k-1} &= (1 - \eta_{k-1})f_k + \eta_{k-1}(1 - \eta_{k-2})f_{k-1} + \dots + \eta_{k-1} \dots \eta_{k-N}f_{k-N} \\ &\quad - \eta_{k-1}(1 - \eta_{k-2})f_{k-1} - \dots - \eta_{k-1} \dots (1 - \eta_{k-N-1})f_{k-N} - \eta_{k-1}\eta_{k-2} \dots \eta_{k-N-1}f_{k-N-1} \\ &= (1 - \eta_{k-1})f_k + \eta_{k-1}\eta_{k-2} \dots \eta_{k-N-1}(f_{k-N} - f_{k-N-1}) \\ &= (1 - \eta_{k-1})f_k + \xi_k(f_{k-N} - f_{k-N-1}), \end{aligned}$$

where $\xi_k := \eta_{k-1}\eta_{k-2} \dots \eta_{k-N-1}$. Thus, for $k \geq N$, this equation leads to

$$\bar{T}_k = (1 - \eta_{k-1})f_k + \eta_{k-1}\bar{T}_{k-1} + \xi_k(f_{k-N} - f_{k-N-1}), \quad (11)$$

which requires to save only f_{k-N} and f_{k-N-1} and needs three multiplications to be updated. The definition of ξ_k implies

$$\xi_k = \eta_{k-1} \eta_{k-2} \cdots \eta_{k-N-1} = \frac{\eta_{k-1}}{\eta_{k-N-2}} \eta_{k-2} \eta_{k-3} \cdots \eta_{k-N-2} = \frac{\eta_{k-1}}{\eta_{k-N-2}} \xi_{k-1}. \quad (12)$$

If ξ_k is recursively updated by (12), then (9) and (11) imply that the new nonmonotone term can be specified by

$$T_k := \begin{cases} f_k + \eta_{k-1}(\bar{T}_k - f_k) & \text{if } k < N; \\ \max \{\bar{T}_k, f_k\} & \text{if } k \geq N, \end{cases} \quad (13)$$

where the max term guaranteeing $T_k \geq f_k$.

As discussed in Section 1, a nonmonotone method performs better whenever it uses a stronger nonmonotone term far away from the optimizer and uses weaker term close to it. This fact motivates us to consider a new version of the derived nonmonotone term by employing $f_{l(k)}$ in the case $k < N$. More precisely, the second nonmonotone term is defined by

$$T_k = \begin{cases} f_{l(k)} & \text{if } k < N; \\ \max \{\bar{T}_k, f_k\} & \text{if } k \geq N, \end{cases} \quad (14)$$

where ξ_k is defined by (12). It is clear that the new term uses stronger term $f_{l(k)}$ defined by (4) for the first $k < N$ iterations and then employs the relaxed convex term proposed above.

We now incorporate the two novel nonmonotone terms into Armijo's line search and outline the subsequent algorithm:

Algorithm 2: NMLS (novel nonmonotone Armijo-type line search algorithm)

Input: $x_0 \in \mathbb{R}^n$, $\rho \in (0, 1)$, $\sigma \in (0, \frac{1}{2})$, $s \in (0, 1]$, $\eta_0 \in [0, 1)$, $\epsilon > 0$, $N \geq 0$;

Output: x_b ; f_b ;

begin

$k \leftarrow 0$; compute f_0 ;
 $T_0 \leftarrow f_0$;
while $\|g_k\| \geq \epsilon$ **do**
 generate a descent direction d_k ;
 $\alpha \leftarrow s$;
 $\hat{x}_k \leftarrow x_k + \alpha d_k$;
 while $f(\hat{x}_k) > T_k + \sigma \alpha g_k^T d_k$ **do**
 $\alpha \leftarrow \rho \alpha$;
 $\hat{x}_k \leftarrow x_k + \alpha d_k$;
 end
 $x_{k+1} \leftarrow \hat{x}_k$;
 choose $\eta_{k+1} \in [0, 1)$;
 update ξ_{k+1} by (12);
 update T_{k+1} by (13) or (14);
 $k \leftarrow k + 1$;
end
 $x_b \leftarrow x_k$, $f_b \leftarrow f_k$;

end

Notice that Algorithm 2 is a simple backtracking line search producing an ϵ -solution x_b satisfying $\|g_b\| < \epsilon$. However, the novel nonmonotone Armijo-type line search can be employed as a part of more sophisticated line searches like Wolfe, strong Wolfe and Goldstein line searches, see [38].

Throughout the paper, we suppose that the following classical assumptions hold in order to verify the global convergence of Algorithm 2:

(H1) The upper level set $L(x_0) = \{x \in \mathbb{R}^n \mid f(x) \leq f(x_0), x \in \mathbb{R}^n\}$ is bounded.

(H2) The gradient of f is Lipschitz continuous over an open convex set C containing $L(x_0)$, i.e., there exists a positive constant L such that

$$\|g(x) - g(y)\| \leq L\|x - y\| \quad \forall x, y \in C.$$

(H3) There exist constants $0 < c_1 < 1 < c_2$ such that the direction d_k satisfies the next conditions

$$g_k^T d_k \leq -c_1 \|g_k\|^2, \quad \|d_k\| \leq c_2 \|g_k\|, \quad (15)$$

for all $k \in \mathbb{N} \cup \{0\}$.

Note that the assumptions (H1) and (H2) are popular assumptions frequently used to establish the global convergence of the sequence $\{x_k\}$ generated by descent methods. There are several possible ways to determine the direction d_k satisfying (15). For example, the gradient descent direction and some kind of spectral gradient direction and conjugate gradient directions are satisfying these conditions, see [3, 45]. Newton and quasi-Newton directions can satisfy (15) with some more assumptions, see [24, 25]. In practice, if Algorithm 2 uses Newton-type or quasi-Newton directions, and one condition of (15) is not satisfied, then one of the gradient-based directions satisfied these conditions can be used in this iteration. In view of rounding error, sometimes the directions generated by Algorithms 2 may not be descent so that if $g_k^T d_k > -10^{-14}$, one can take a advantage of the gradient descent direction instead.

We now verify the global convergence of the sequence gradient $\{x_k\}$ generated by Algorithm 2. Thanks to the similarity of the convergence proof of the current study and those reported in [4, 6], we refer most of proofs to the related results of these literatures to avoid the repetition.

Lemma 3 Suppose that the sequence $\{x_k\}$ is generated by Algorithm 2, then we have

$$f_k \leq T_k \leq f_{l(k)}, \quad (16)$$

for all $k \in \mathbb{N} \cup \{0\}$.

Proof For $k \leq N$, we divide the proof into two cases: (i) T_k defined by (13); (ii) T_k defined by (14). For Case (i), Lemma 2.1 in [4] implies $f_k \leq f_{l(k)}$ for $i = 0, 1, \dots, k$, and since summation of multipliers in T_k equal to one give the result. Case (ii) is deduced from (14).

For $k \geq N$, if $T_k = f_k$, then the result is evident. Otherwise, (10), (13) and the fact that $f_k \leq f_{l(k)}$ for $i = k - N + 1, \dots, k$ imply

$$\begin{aligned} f_k &\leq T_k = (1 - \eta_{k-1}) f_k + \eta_{k-1} (1 - \eta_{k-2}) f_{k-1} + \dots + \eta_{k-1} \dots \eta_{k-N} f_{k-N} \\ &\leq [(1 - \eta_{k-1}) + \eta_{k-1} (1 - \eta_{k-2}) + \dots + \eta_{k-1} \dots \eta_{k-N}] f_{l(k)} = f_{l(k)}, \end{aligned}$$

giving the result.

Lemma 4 Suppose that (H1) and (H2) hold, and let the sequence $\{x_k\}$ be generated by Algorithm 2, then we have

$$\lim_{k \rightarrow \infty} T_k = \lim_{k \rightarrow \infty} f(x_k). \quad (17)$$

Proof From (16) and Lemma 2 of [6], the result is valid.

Lemma 5 Suppose that the sequence $\{x_k\}$ be generated by Algorithm 2. Then, the new nonmonotone line search is well-defined. Moreover, if $\tilde{\alpha}$ and α are step-sizes generated by monotone Armijo's rule (2) and the nonmonotone line search of Algorithm 2, respectively, then $\tilde{\alpha} \leq \alpha$.

Proof Using (16) and similar to Lemma 2.3 of [4], the results hold.

Theorem 6 Suppose that (H1), (H2) and (H3) hold, and let the sequence $\{x_k\}$ is generated by Algorithm 2. Then, we have

$$\lim_{k \rightarrow \infty} \|g_k\| = 0. \quad (18)$$

Furthermore, there is not any limit point of the sequence $\{x_k\}$ that be a local maximum of $f(x)$.

Proof By similar proofs of Lemma 3 and Theorem 1 of [6], the results are valid.

Theorem 6 suggests that the sequence $\{x_k\}$ generated by Algorithm 2 is globally convergent to a first-order stationary point of (1). The R -linearly convergence of the sequence $\{x_k\}$ for strongly convex objective function can be proved the same as Lemma 4.1 and Theorem 4.2 in [4]. Furthermore, if the algorithm exploits quasi-Newton or Newton directions, the superlinear or quadratic convergence rate also can be established similar to Theorem 4.3 and Theorem 4.4 of [4] by a slight modification.

3 Numerical experiments and comparisons

This section reports some numerical results of our experiments with Algorithm 2 using the two novel nonmonotone terms to verify and assess their efficiency for solving unconstrained optimization problems. In our experiments, we first consider modified versions of damped Newton's method, Algorithm 2 with Newton's direction, and the BFGS method, Algorithm 2 with the BFGS direction, using various nonmonotone terms for solving some small-scale test problems. Afterwards, versions of Algorithm 2 equipped with the novel nonmonotone terms and LBFGS and Barzilai-Borwein directions are performed on a large set of test problems, and their performance are compared to some state-of-the-art algorithms.

In the experiment with damped Newton's method and the BFGS method, we only consider 18 unconstrained test problems from MORÉ et al. in [33], while in implementation of Algorithm 2 with LBFGS and Barzilai-Borwein directions a set of 94 standard test functions from ANDREI in [8] and MORÉ et al. in [33] is used. In our comparisons, we employ the following algorithms:

- NMLS-G: the nonmonotone line search of GRIPPO et al. [25];
- NMLS-H: the nonmonotone line search of ZHANG & HAGER [45];
- NMLS-N: the nonmonotone line search of AMINI et al. [6];
- NMLS-M: the nonmonotone line search of AHOOKHOSH et al. [3];
- NMLS-1: a version of Algorithm 2 using the nonmonotone term (14);
- NMLS-2: a version of Algorithm 2 using the nonmonotone term (13);

All of these codes are written in MATLAB using the same subroutine, and they are tested on 2Hz core i5 processor laptop with 4GB of RAM with double precision format. The initial points are standard ones reported in [8] and [33]. All the algorithms use the parameters $\rho = 0.5$ and $\sigma = 0.01$. For NMLS-N, NMLS-G, NMLS-1 and NMLS-2, we set $N = 10$. As discussed in [45], NMLS-H uses $\eta_k = 0.85$. On the basis of our experiments, we update the parameter η_k adaptively by

$$\eta_k = \begin{cases} \eta_0/2 & \text{if } k = 1; \\ (\eta_{k-1} + \eta_{k-2})/2 & \text{if } k \geq 2, \end{cases} \quad (19)$$

for NMLS-N, NMLS-M, NMLS-1 and NMLS-2, where the parameter η_0 will be tuned to get a better performance. In our experiments, the algorithms are stopped whenever the total number of iterates exceeds `maxiter = 50000` or

$$\|g_k\| < \epsilon \quad (20)$$

holds with the accuracy parameter $\epsilon = 10^{-5}$. We further declare an algorithm "failed" if the maximum number of iterations is reached.

To compare the results appropriately, we use the performance profiles of DOLAN & MORÉ in [23], where the measures of performance are the number of iterations (N_i), function evaluations (N_f) and gradient evaluations (N_g). It is clear that in the considered algorithms the number of iterations and gradient evaluations are the same, so we only consider the performance of gradients. It is believed that computing a gradient is as costly as computing three function values, i.e., we further consider the measure $N_f + 3N_g$. In details, the performance of each code is measured by considering the ratio of its computational outcome versus the best numerical outcome of all codes. This profile offers a tool for comparing the performance of iterative processes in a statistical structure. Let \mathcal{S} be a set of all algorithms and \mathcal{P} be a set of test problems. For each problem p and solver s , $t_{p,s}$ is the computational outcome regarding to the performance index, which is used in defining the next performance ratio

$$r_{p,s} = \frac{t_{p,s}}{\min\{t_{p,s} : s \in \mathcal{S}\}}. \quad (21)$$

If an algorithm s is failed to solve a problem p , the procedure sets $r_{p,s} = r_{failed}$, where r_{failed} should be strictly larger than any performance ratio (21). For any factor τ , the overall performance of a algorithm s is given by

$$\rho_s(\tau) = \frac{1}{n_p} \text{size}\{p \in \mathcal{P} : r_{p,s} \leq \tau\}.$$

In fact $\rho_s(\tau)$ is the probability that a performance ratio $r_{p,s}$ of the algorithm $s \in \mathcal{S}$ is within a factor $\tau \in \mathbf{R}^n$ of the best possible ratio. The function $\rho_s(\tau)$ is a distribution function for the performance ratio. In particular, $\rho_s(1)$ gives the probability that an algorithm s wins over all other considered algorithms,

and $\lim_{\tau \rightarrow r_{failed}} \rho_s(\tau)$ gives the probability of that algorithm s solve all considered problems. Therefore, this performance profile can be considered as a measure of efficiency among all considered algorithms. In Figures 1-4, the x-axis shows the number τ while the y-axis inhibits $P(r_{p,s} \leq \tau : 1 \leq s \leq n_s)$.

3.1 Experiments with damped Newton and BFGS

In this section, we report numerical results of solving the problem (1) by NMLS-G, NMLS-H, NMLS-N, NMLS-M, NMLS-1 and NMLS-2 using damped Newton and BFGS directions and compare their performance. Since both damped Newton and BFGS methods require to solve a linear system of equations in each iteration, it is expected to solve large-scale problems with them. Thus we only consider 18 small-scale test problems from MORÉ [33] with their standard initial points. For NMLS-1 and NMLS-2, we use $\eta_0 = 0.75$. The results for damped Newton's method and the BFGS method are summarized in Tables 1 and 2, respectively.

Table 1 and 2 show that the results are comparable for the considered algorithms, however NMLS-1 and NMLS-2 perform slightly better. To see the results of implementations in details, we illustrate the results with performance profile in Figure 3 with N_g , N_f and $N_f + 3N_g$ as measures of performance. Subfigures (a), (c) and (e) of Figure 3 show the results of damped Newton's method, while subfigures (b), (d) and (f) of Figure 3 demonstrate the results of the BFGS method.

3.2 Experiments with LBFGS

In the recent decades, the interest for solving optimization problems with large number of variables is remarkably increased thanks to the dramatic emerge of big data in science and technology. This section devotes to an experiment with the considered algorithms with LBFGS which is the limited memory version of the BFGS scheme, and that is much more appropriate for solving large problems, see [30, 39].

The LBFGS scheme calculates a search direction by $d_k = -H_k g_k$, where H_k is an approximate of inverse Hessian determined by

$$\begin{aligned} H_{k+1} = & (V_k^T \cdots V_{k-m}^T) H_0 (V_{k-m} \cdots V_k) \\ & + \rho_{k-m} (V_k^T \cdots V_{k-m+1}^T) s_{k-m} s_{k-m}^T (V_{k-m+1} \cdots V_k) \\ & + \rho_{k-m+1} (V_k^T \cdots V_{k-m+2}^T) s_{k-m+1} s_{k-m+1}^T (V_{k-m+2} \cdots V_k) \\ & \vdots \\ & + \rho_k s_k s_k^T, \end{aligned}$$

in which $\rho_k = 1/y_k^T s_k$ and $V_k = I - \rho_k y_k s_k^T$. The scheme starts from a symmetric positive definite initial matrix H_0 and sets $m = \min\{k, 10\}$. Indeed, it does not need to save the previous approximate matrix, instead it employs only small number of former information to construct the new search direction d_k . This causes that the method needs much less memory compared with the original BFGS method making it suitable for solving large-scale problems. The LBFGS code is publicly available from [44], however, we rewrite it in MATLAB.

It is believed that nonmonotone algorithms perform better when they employ a stronger nonmonotone term far away from the optimizer and a weaker term close to it. Hence, to get the best performance of the proposed algorithms, we first conduct some test to find a better starting parameter for η_0 in the adaptive process (19). To this end, for both algorithms NMLS-1 and NMLS-2, we consider cases that the algorithms start from $\eta_0 = 0.65$, $\eta_0 = 0.75$, $\eta_0 = 0.85$ and $\eta_0 = 0.95$. The corresponding versions of algorithms NMLS-1 and MNLS-2 are denoted by NMLS-1-0.65, NMLS-1-0.75, NMLS-1-0.85, NMLS-1-0.95, NMLS-2-0.65, NMLS-2-0.75, NMLS-2-0.85 and NMLS-2-0.95, respectively. The results of this test are summarized in Figure 4.

In Figure 4, subfigures (a), (c) and (e) suggest that the results of NMLS-1 with $\eta_0 = 0.75$ are considerably better than those reported for others parameters regarding all of considered measures. In particular, it wins 77%, 73% and 75% score among others for N_i , N_f and $N_f + 3N_g$, respectively. The same results for NMLS-2 in subfigures (b), (d) and (f) of Figure 4 can be observed, where NMLS-2-0.75 respectively wins in 70%, 71% and 70% of the cases for the considered measures. Therefore, we consider

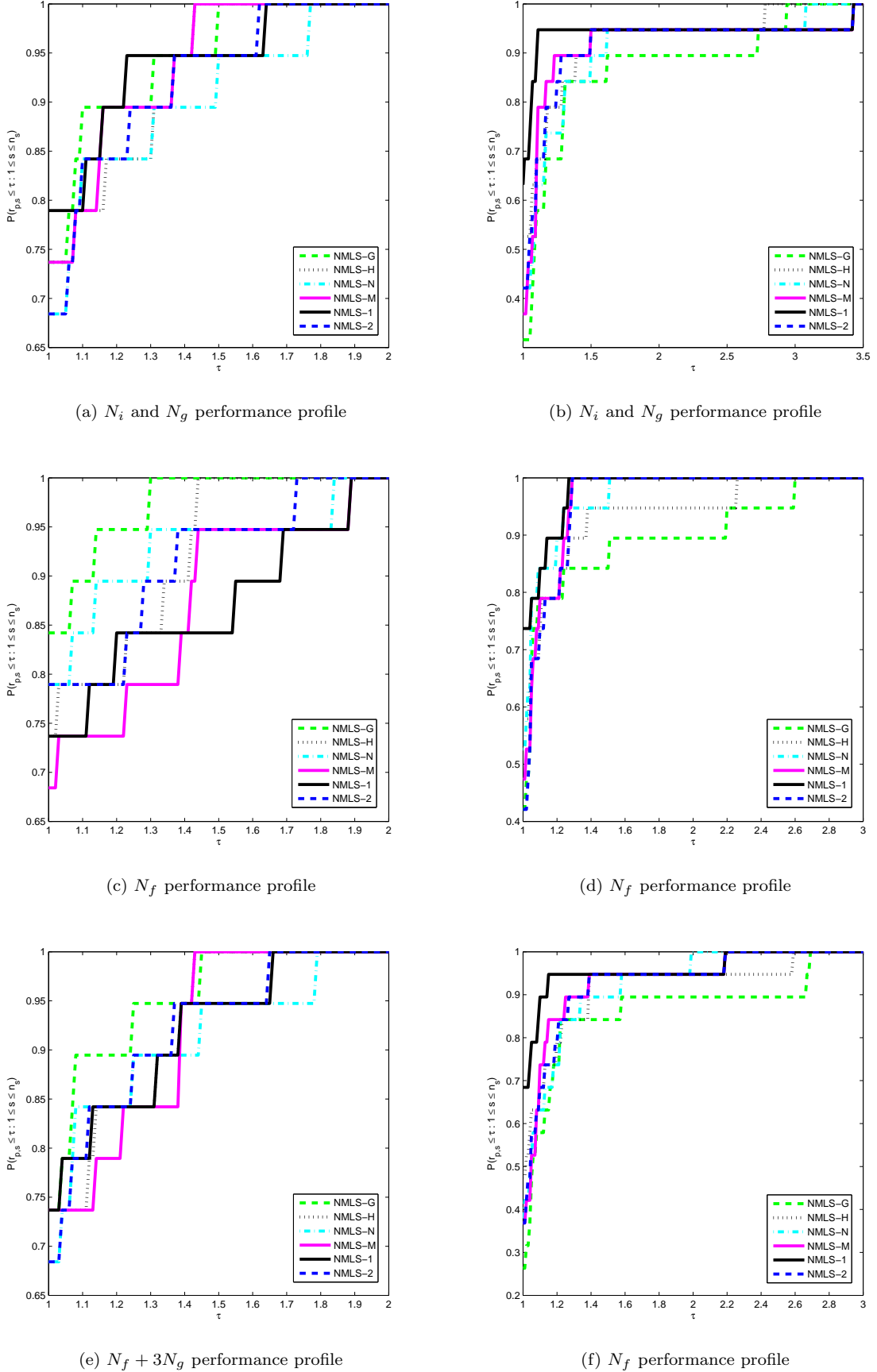


Fig. 3: Performance profiles of all considered algorithms with the performance measures: (a) and (b) for the number of iterations (N_i) or gradient evaluations (N_g); (c) and (d) for the number of function evaluations (N_f); (e) and (f) for the hybrid measure $N_f + 3N_g$.

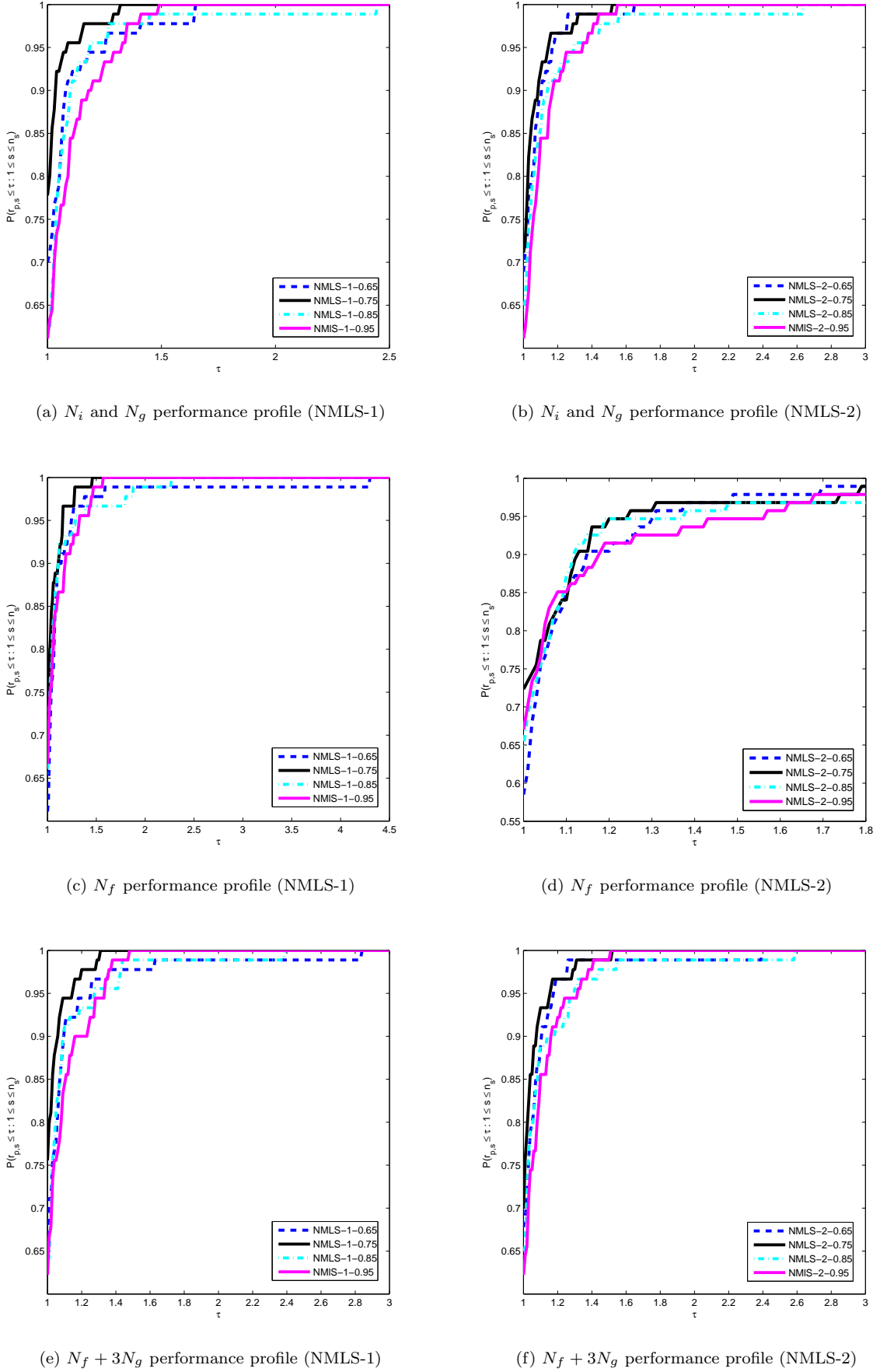


Fig. 4: Performance profiles of NMLS-1 and NMLS-2 with the performance measures: (a) and (b) for the number of iterations (N_i) or gradient evaluations (N_g); (c) and (d) for the number of function evaluations (N_f); (e) and (f) for the hybrid measure $N_f + 3N_g$.

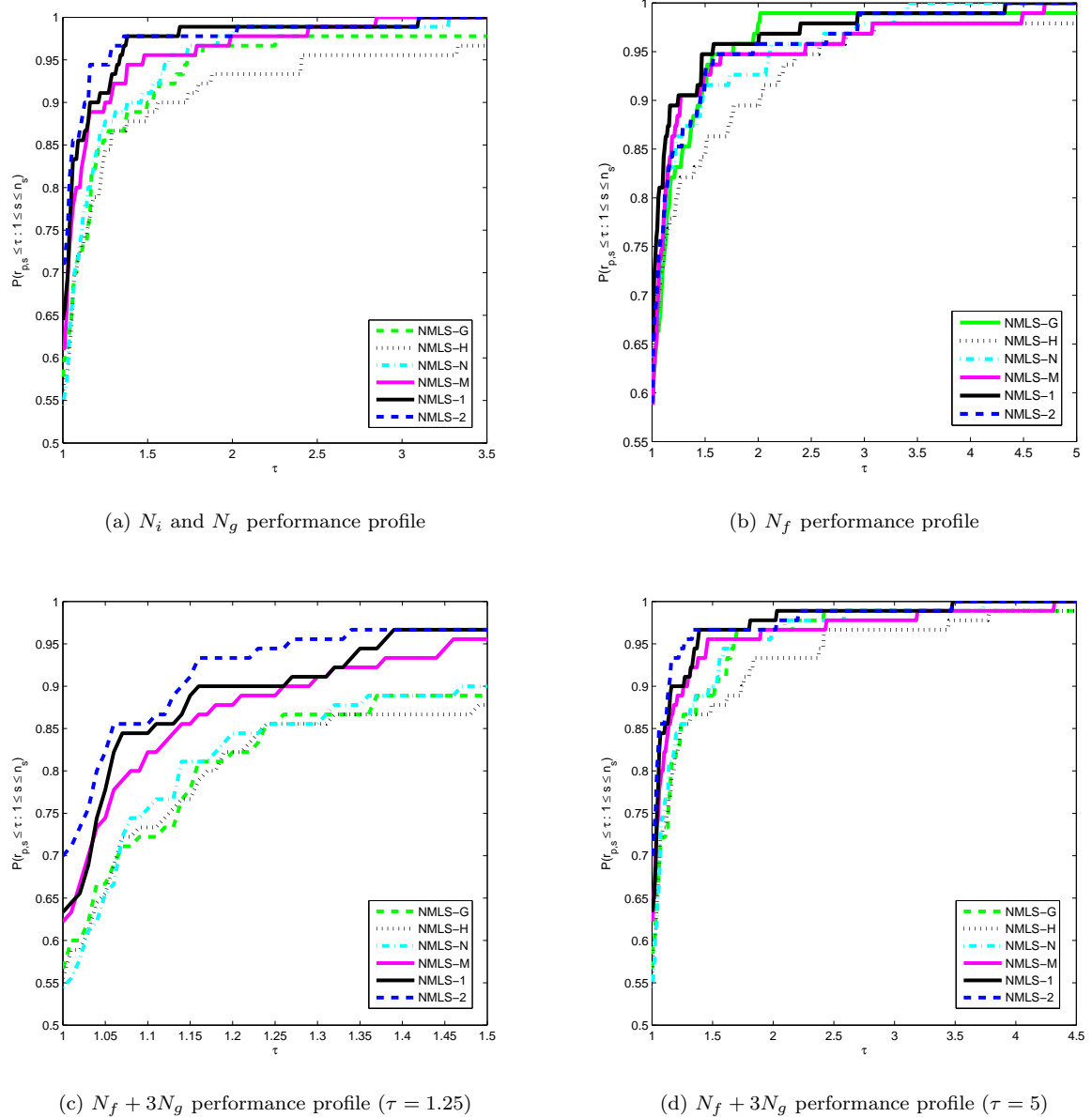


Fig. 5: Performance profiles of all considered algorithms measured by: (a) the number of iterations (N_i) or gradient evaluations (N_g); (b) the number of function evaluations (N_f); (c) and (d) the hybrid measure $N_f + 3N_g$.
 $\eta_0 = 0.75$ for our algorithms and for the sake of simplicity denote NMLS-1-0.75 and NMLS-2-0.75 by NMLS-1 and NMLS-2 in the rest of the paper.

In this point, we test NMLS-G, NMLS-H, NMLS-R, NMLS-M, NMLS-1 and NMLS-2 to solve the problem (1) by the LBFGS direction. Results of implementation are illustrated in Figure 5. From subfigure (a) of Figure 5, NMLS-2 obtains the most wins by 71%, then NMLS-1 has the next place by 64%. Moreover, NMLS-1 and NMLS-2 solve all problems in about $\tau = 3.8$. The subfigure (b) of Figure 5 demonstrates the number of function evaluations suggesting the similar results discussed about the subfigure (a). In Figure 5, subfigures (c) and (d) illustrate the performance profile of the algorithms with the measure $N_f + 3N_g$ by different amount of τ indicating that NMLS-1 and NMLS-2 win by 63% and 70% score among others, and they also solve the problems in less amount of τ .

3.3 Experiment with Barzilai-Borwein

The Barzilai-Borwein (BB) method for solving the problem (1) is a gradient-type method proposed by BARZILAI & BORWEIN in [10], where a step-size along the gradient descent direction $-g_k$ is generated using a two-point approximation of the secant equation $B_k s_{k-1} = y_{k-1}$ with $s_{k-1} = x_{k-1} - x_{k-2}$ and $y_{k-1} = g_{k-1} - g_{k-2}$. In particular, by imposing $B_k = \sigma_k I$ and solving the least-squares problem

$$\begin{aligned} & \text{minimize} && \|\sigma s_{k-1} - y_{k-1}\|_2^2 \\ & \text{subject to} && \sigma \in \mathbb{R}, \end{aligned}$$

one can obtain

$$\sigma_k^{BB1} = \frac{s_{k-1}^T y_{k-1}}{s_{k-1}^T s_{k-1}}.$$

Hence the two-point approximated quasi-newton direction is computed by

$$d_k = -(\sigma_k^{BB1})^{-1} g_k = -\frac{s_{k-1}^T s_{k-1}}{s_{k-1}^T y_{k-1}} g_k.$$

Since σ_k in this direction can be unacceptably small or large for non-quadratic objective function, we use the following safeguarded step-size

$$d_k^{BB1} = \begin{cases} -(\sigma_k^{BB1})^{-1} g_k & \text{if } 10^{-10} \leq (\sigma_k^{BB1})^{-1} \leq 10^{10}, \\ -g_k & \text{otherwise.} \end{cases} \quad (22)$$

Similarly, setting $B_k^{-1} = \frac{1}{\sigma_k} I$ and solving the minimization problem

$$\begin{aligned} & \text{minimize} && \|s_{k-1} - \frac{1}{\sigma} y_{k-1}\|_2^2 \\ & \text{subject to} && \sigma \in \mathbb{R}, \end{aligned}$$

we obtain the step-size

$$\sigma_k^{BB2} = \frac{y_{k-1}^T s_{k-1}}{y_{k-1}^T y_{k-1}}.$$

Considering the safeguard used in (22), we obtain the following search direction

$$d_k^{BB2} = \begin{cases} -(\sigma_k^{BB2})^{-1} g_k & \text{if } 10^{-10} \leq (\sigma_k^{BB2})^{-1} \leq 10^{10}, \\ -g_k & \text{otherwise.} \end{cases} \quad (23)$$

The numerical experiments with the Barzilai-Borwein directions have shown the significant development in efficiency of gradient methods. Being computationally efficient and needing low memory requirement make this scheme interesting to solve large-scale optimization problems. Therefore, it receives much attention during the last two decades and lots of modifications and developments for both unconstrained and constrained optimization have been proposed, for example see [7, 12, 13, 20, 21, 22, 28, 29, 31, 42] and references therein.

In the rest of this subsection, we consider versions of Algorithm 2 equipped with the nonmonotone terms using the Barzilai-Borwein directions (22) and (23) for solving the problem (1). We here set $\sigma = 10^{-4}$. To find the best possible parameter η_0 , we consider $\eta_0 = 0.65$, $\eta_0 = 0.75$, $\eta_0 = 0.80$ and $\eta_0 = 0.90$ and run NMLS-1 and NMLS-2 for both directions (22) and (23). The corresponding results are summarized in Figures 6 and 7, where the first row shows the performance profile for the number of gradients N_g , the second row shows the performance profile for the number of function evaluations N_f and the third row shows the performance profile for $N_f + 3N_g$. From all subfigures of Figures 6 and 7, we conclude that $\eta_0 = 0.80$ and $\eta_0 = 0.90$ produce acceptable results for our algorithms with respect to the directions (22) and (23), i.e., NMLS-1 and NMLS-2 exploit $\eta_0 = 0.80$ and $\eta_0 = 0.90$ for these directions, respectively.

We now compare the performance of NMLS-G, NMLS-H, NMLS-N and NMLS-M, NMLS-1 and NMLS-2 using the directions (22) and (23). The test problems are those considered in the previous subsection. The related results are gathered in Tables 4 and 5. All considered algorithms are failed for some test problems in our implementation, WASTON, HARKAPER2, POWER, Extended HILBERT, FLETCHER,

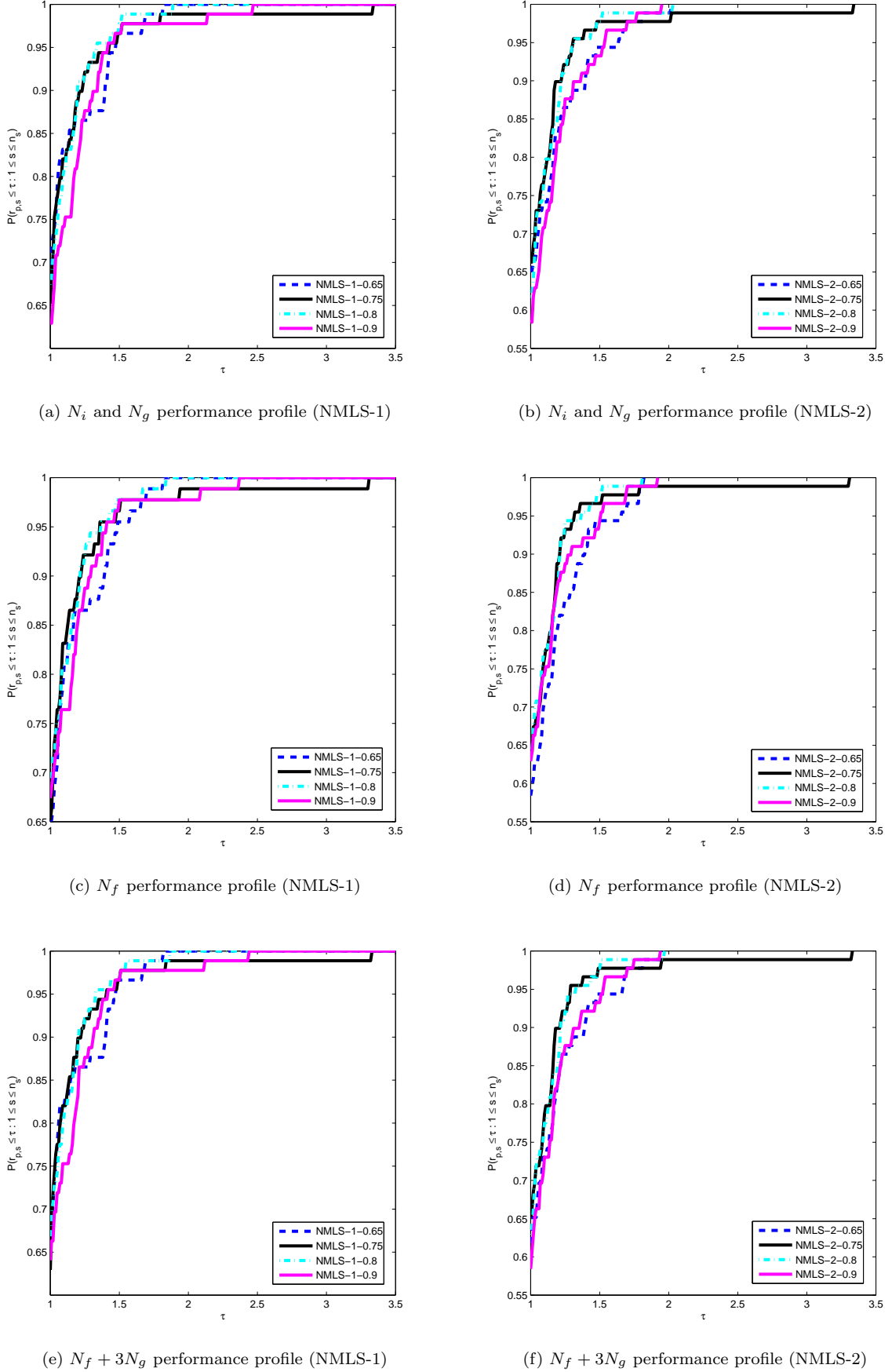


Fig. 6: Performance profiles of NMLS-1 and NMLS-2 with the performance measures: (a) and (b) for the number of iterations (N_i) or gradient evaluations (N_g); (c) and (d) for the number of function evaluations (N_f); (e) and (f) for the hybrid measure $N_f + 3N_g$.

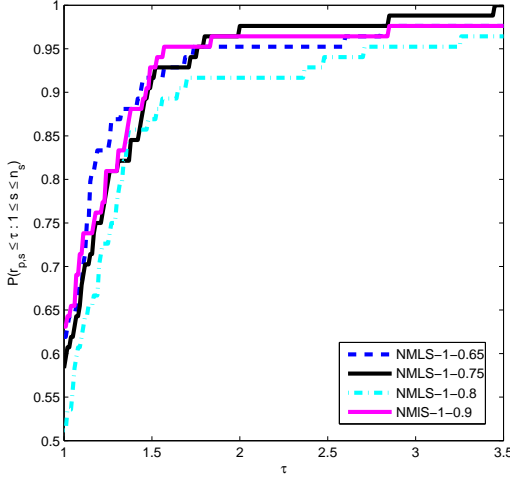
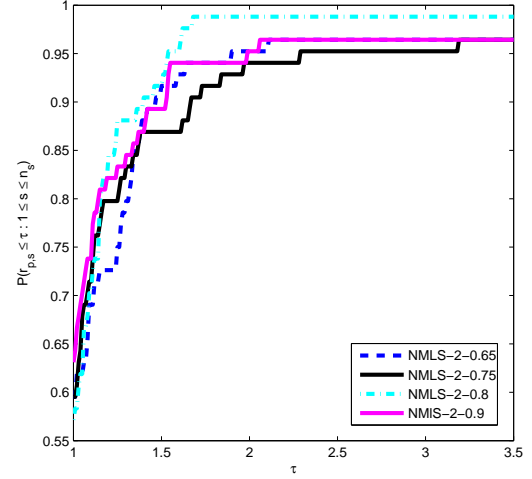
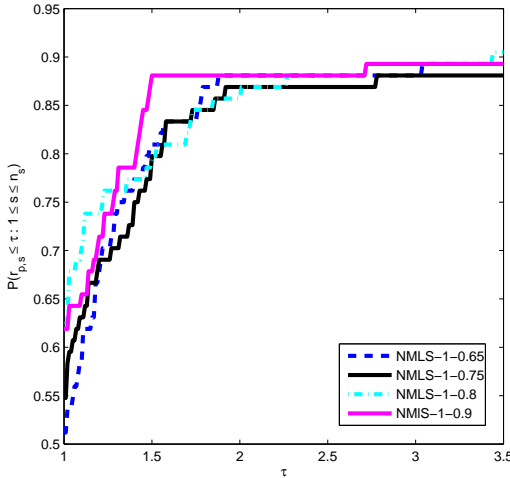
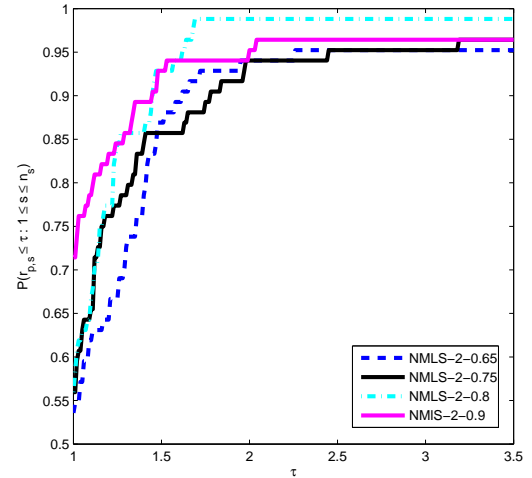
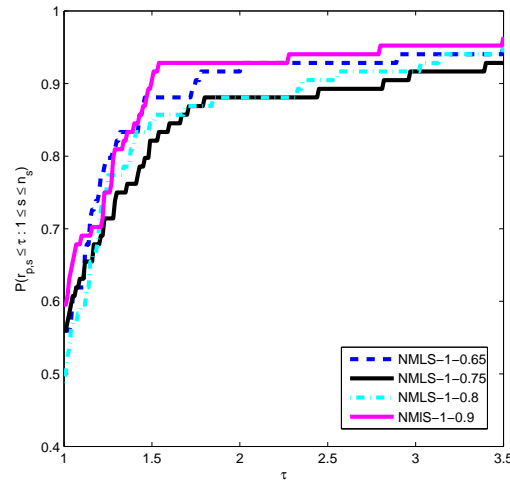
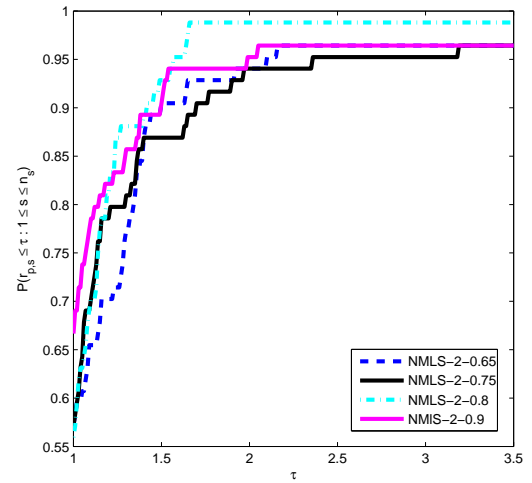
(a) N_i and N_g performance profile (NMLS-1)(b) N_i and N_g performance profile (NMLS-2)(c) N_f performance profile (NMLS-1)(d) N_f performance profile (NMLS-2)(e) $N_f + 3N_g$ performance profile (NMLS-1)(f) $N_f + 3N_g$ performance profile (NMLS-2)

Fig. 7: Performance profiles of NMLS-1 and NMLS-2 with the performance measures: (a) and (b) for the number of iterations (N_i) or gradient evaluations (N_g); (c) and (d) for the number of function evaluations (N_f); (e) and (f) for the hybrid measure $N_f + 3N_g$.

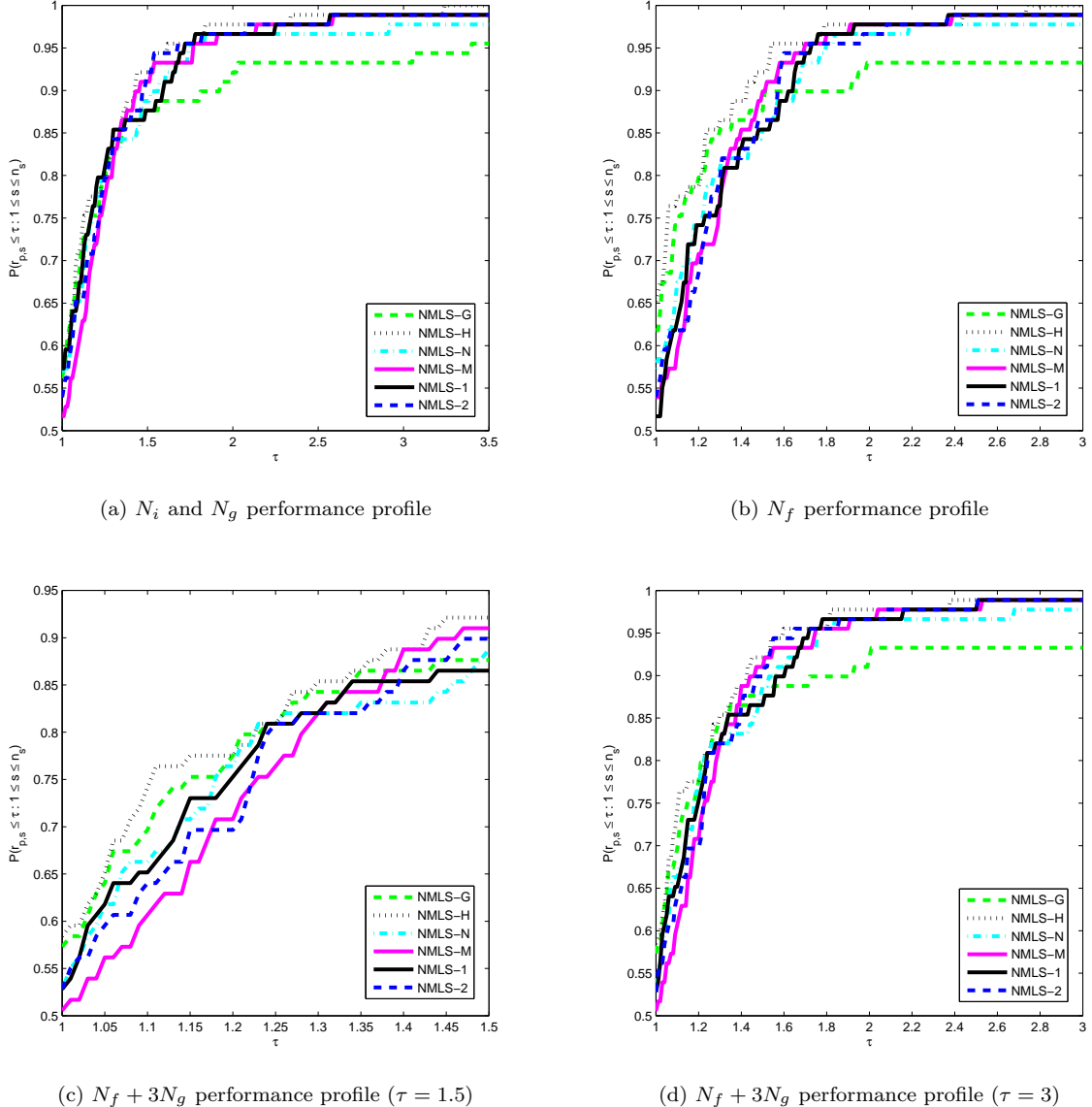


Fig. 8: Performance profiles of all considered algorithms measured by: (a) the number of iterations (N_i) or gradient evaluations (N_g); (b) the number of function evaluations (N_f); (c) and (d) the hybrid measure $N_f + 3N_g$.

CUBE and Generalized White and Holst for (22) and CUBE and Generalized White and Holst for (23), so we delete them from Tables 4 and 5. The performance profile of the algorithms are demonstrated in Figures 8 and 9 for the measures N_g , N_f and $N_f + 3N_g$. Subfigures (a) and (b) of Figure 8 respectively illustrate the performance profile for N_g and N_f and indicate that the algorithms are comparable, however, NMLS-G and NMLS-H perform a little better regarding the number of function values. Subfigures (c) and (d) stand for the measure $N_f + 3N_g$ with $\tau = 1.5$ and $\tau = 3$, respectively. They show that MNLS-H attains the most wins by about 58% and then NMLS-G by 57% while NMLS-N, NMLS-1 and NMLS-2 attain about 53% score of the wins and NMLS-M get the worst result by about 50%. Similarly, subfigures (a) and (b) of Figure 9 demonstrate the performance profile for N_g and N_f , where they are comparable regarding the number of gradient evaluations, and NMLS-H and NMLS-G perform better regarding the number of function evaluations. Subfigures (c) and (d) of Figure 9 show that NMLS-H, MNLS-G and NMLS-1 attain the most wins by about 49%, 48% and 47% score, respectively.

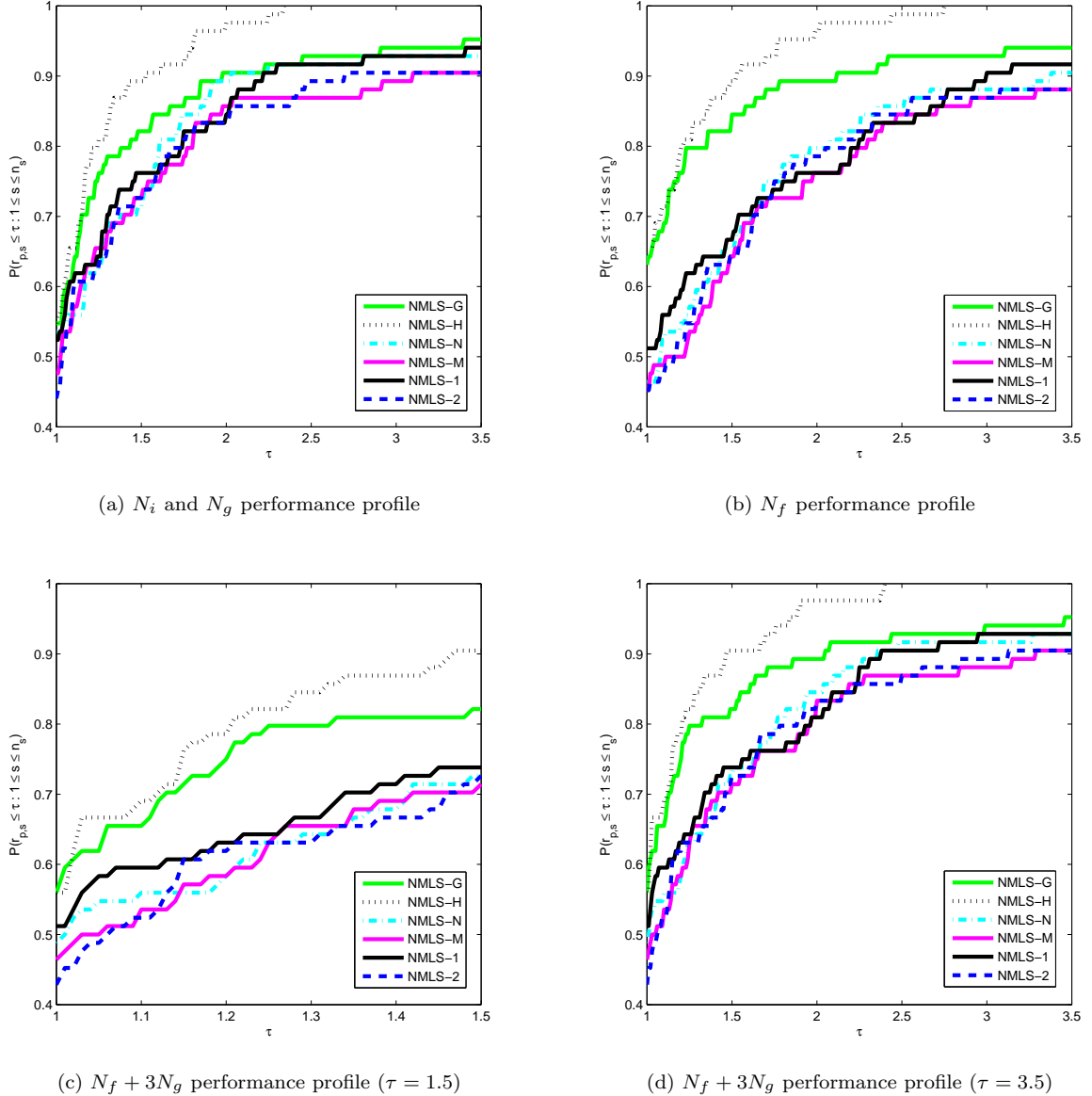


Fig. 9: Performance profiles of all considered algorithms measured by: (a) the number of iterations (N_i) or gradient evaluations (N_g); (b) the number of function evaluations (N_f); (c) and (d) the hybrid measure $N_f + 3N_g$.

Summarizing the results of this subsection, we see that the considered algorithms are comparable, however, NMLS-H and NMLS-G attain the best performance by using the direction (22), while NMLS-H, NMLS-G and NMLS-1 outperform the others by employing the direction (23).

3.4 Image deblurring/denoising

Image blur is a common problem that frequently happens in the photography and often can ruin the photograph. In digital photography, the motion blur is caused by camera shakes, which is unavoidable in many situations. Hence image deblurring/denoising is one of the fundamental tasks in the context of digital imaging processing, aiming at recovering an image from a blurred/noisy observation. The problem is typically modelled as linear inverse problem

$$y = Ax + \omega, \quad x \in X, \quad (24)$$

where X is a finite-dimensional vector space, A is a blurring linear operator, x is a clean image, y is an observation, and ω is either Gaussian or impulsive noise.

The system of equations (24) is mostly underdetermined and ill-conditioned, and ω is not commonly available, so one is not able to solve it directly, see [11, 36]. Hence, its solution is generally approximated by an optimization problem of the form

$$\begin{aligned} & \text{minimize} && \frac{1}{2} \|Ax - y\|_2^2 + \lambda \varphi(x) \\ & \text{subject to} && x \in X, \end{aligned} \quad (25)$$

where φ is a smooth or nonsmooth regularizer such as $\varphi(x) = \frac{1}{2}\|x\|_2^2$, $\varphi(x) = \|x\|_1$, $\varphi(x) = \|x\|_{ITV}$, or $\varphi(x) = \|x\|_{ATV}$ in which $\|\cdot\|_{ITV}$ and $\|\cdot\|_{ATV}$ denote isotropic and anisotropic total variation, for more information see [1, 18] and references therein. Among these regularizers, $\varphi(x) = \frac{1}{2}\|x\|_2^2$ is differentiable and the others are nondifferentiable. Therefore, by the aim of this paper to study differentiable objective function, we consider the next problem

$$\begin{aligned} & \text{minimize} && \frac{1}{2} \|Ax - y\|_2^2 + \frac{\lambda}{2} \|Wx\|_2^2 \\ & \text{subject to} && x \in \mathbb{R}^n, \end{aligned} \quad (26)$$

where $A, W \in \mathbb{R}^{m \times n}$ and $y \in \mathbb{R}^m$. It is assumed that $A^T A + \lambda W^T W$ is positive definite, i.e., the problem (26) is a strictly convex problem and has the unique optimizer $x^* \in \mathbb{R}^n$ for an arbitrary vector y .

We now consider the recovery of the 256×256 blurred/noisy Lena image by minimizing the problem (26) using NMLS-G, NMLS-H, NMLS-N, NMLS-M, NMLS-1 and NMLS-2 with the search direction (23). The algorithms stopped after 25 iterations. In particular, we choose the blurring matrix $A \in \mathbb{R}^{n \times n}$ to be the out-of-focus blur with radius 3 and the regularization matrix W to be the gradient matrix for the problem (26). Thus, the matrix $W^T W$ is the two-dimensional discrete Laplacian matrix. For both matrices, we exploit the Neumann boundary conditions, which usually gives less artifacts at the boundary, see [34, 37]. The use of such boundary conditions means that $A^T A + \lambda W^T W$ is a block-Toeplitz-plus-Hankel matrix with Toeplitz-plus-Hankel blocks. The original and blurred/noisy version of Lena are demonstrated in Figure 10, and the recovered images by the considered algorithms of this image are depicted in Figure 12.



(a) Original image

(b) Blurred/noisy image

Fig. 10: The 256×256 original and blurred/noisy Lena images

To see details of this experiment, we compare the function values and signal-to-noise improvement (ISNR) for the algorithms in Figure 11, where ISNR is defined by

$$\text{ISNR} = 20 \log_{10} \left(\frac{\|y - x_0\|_2}{\|x_b - x_0\|_2} \right),$$

where y is the observed image. Generally, this ratio measures the quality of the restored image x_b relative to the blurred/noisy observation y . The subfigure (a) of Figure 11 shows that the algorithms perform comparable, while the subfigure (b) of Figure 11 indicates that NMLS-1 and NMLS-2 outperform the other algorithms regarding ISNR.

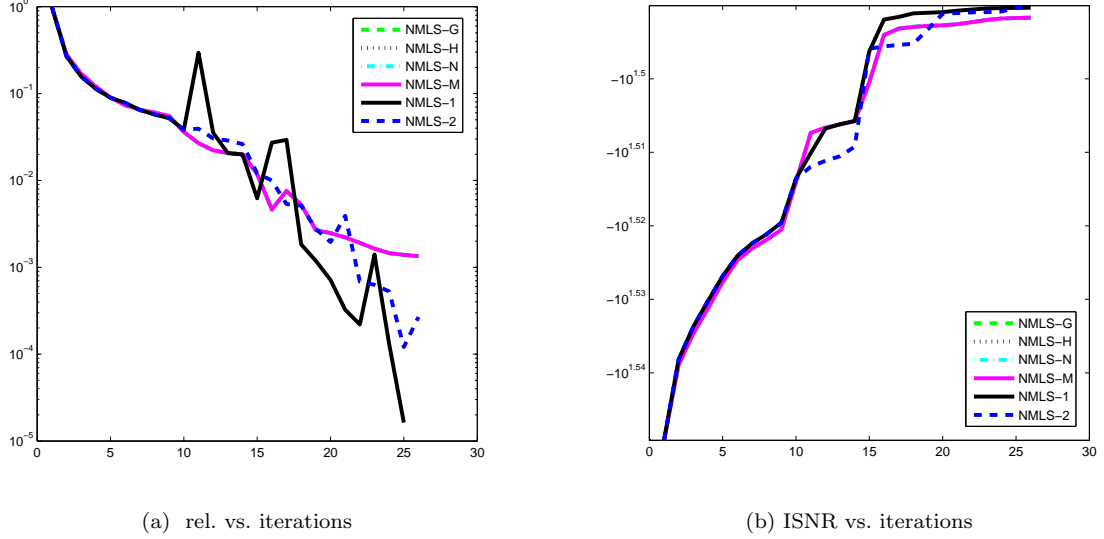


Fig. 11: Deblurring of the 256×256 blurred/noisy image by NMLS-G, NMLS-H, NMLS-N, NMLS-M, NMLS-1 and NMLS-2, where $rel. := (f_k - f^*)/(f_0 - f^*)$ is the relative error of function values.

From Figure 12, it is observed that the algorithms recover the image in acceptable quality, where the last function value and PSNR are also reported. Here peak signal-to-noise (PSNR) is defined by

$$PSNR = 20 \log_{10} \left(\frac{255n}{\|x_b - x_0\|_2} \right),$$

where x_b is the approximated solution of (26) and x_0 is an initial point. This ratio is a common measure to assess the quality of the restored image x_b , i.e., it implies that NMLS-1 and NMLS-2 recover the blurred/noisy image better than the others.

4 Conclusions and perspectives

This study first describes the motivation behind nonmonotone schemes, reviews the most popular non-monotone terms and investigates the efficiency of them when they are incorporated into a backtracking Armijo-type line search in presence of some search directions. In particular, we propose two novel non-monotone terms, combine them with Armijo's rule and study their convergence. Afterwards, we report extensive numerical results and comparison among the two proposed nonmonotone schemes and some state-of-the-art nonmonotone line searches. The reported numerical results by using some measures of efficiency show that the performance of the considered nonmonotone line searches are varied depends on choosing search directions. Finally, employing the nonmonotone Armijo line searches for solving the deblurring problem produces acceptable results.

The experiments of this paper are limited to unconstrained optimization problems, however, the same experiments can be done for bound-constrained or general constrained optimization problems. We here consider only an Armijo-type line search, but one can investigate more numerical experiments with Wolfe-type or Goldestein-type line searches. For example studying of the behaviour of nonmonotone Wolfe-type line searches using conjugate-gradient directions is interesting. Furthermore, much more experiments on the parameters ρ and δ for nonmonotone Armijo-type line searches can be done. It is also possible to extend our experiments to trust-region methods. One can consider many more applications with convex or

nonconvex objective functions in the context of signal and image processing, machine learning, statistics and so on, which is out of the scope of this study.

Acknowledgement. We would like to thank BENEDETTA MORINI that generously makes the codes of the paper [34] available for us.

Appendix: Tables 1–5

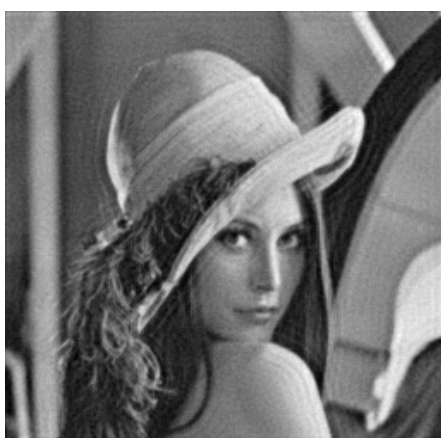
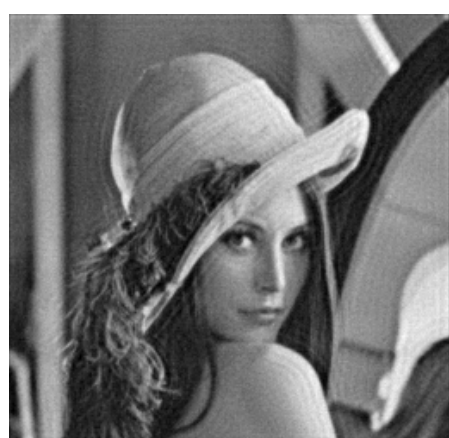
(a) NMLS-G: $f = 50137.53$, PSNR = 29.79(b) NMLS-H: $f = 50137.53$, PSNR = 29.79(c) NMLS-N: $f = 50137.53$, PSNR = 29.79(d) NMLS-M: $f = 50137.53$, PSNR = 29.79(e) NMLS-1: $f = 49445.59$, PSNR = 29.89(f) NMLS-2: $f = 49600.29$, PSNR = 29.90

Fig. 12: Deblurring of the 256×256 blurred/noisy image by NMLS-G, NMLS-H, NMLS-N, NMLS-M, NMLS-1 and NMLS-2. The algorithms were stopped after 25 iterations.

Table 1. Numerical results with Newton's direction

Problem name	Dimension	NMLS-G		NMLS-H		NMLS-N		NMLS-M		NMLS-1		NMLS-2	
		N_i	N_f										
Beale	2	17	25	14	27	17	25	14	27	13	22	16	28
Brown badly scaled	2	7	113	7	113	7	113	7	113	7	113	7	113
Powell badly scaled	2	4	89	4	89	4	89	4	89	4	89	4	89
Variably Dim	2	7	8	7	8	7	8	7	8	7	8	7	8
Watson	2	4	5	4	5	4	5	4	5	4	5	4	5
Box three-dim	3	8	9	8	9	8	9	8	9	8	9	8	9
Gaussian	3	1	2	1	2	1	2	1	2	1	2	1	2
Gulf r. and d.	3	39	46	43	47	39	46	37	47	41	55	39	46
Helical valley	3	21	22	20	24	21	22	20	24	14	19	14	17
Bro. a. Dennis	4	11	66	11	66	11	66	11	66	11	66	11	66
E. Rosenbrock	4	11	16	15	23	11	16	15	23	18	27	15	22
E. Powell singular	4	15	16	15	16	15	16	15	16	15	16	15	16
Penalty I	4	16	17	16	17	16	17	16	17	16	17	16	17
Penalty II	4	8	9	8	9	8	9	8	9	8	9	8	9
Trigonometric	4	8	12	8	12	8	12	8	12	8	12	8	12
Wood	4	29	33	27	31	29	33	31	43	33	48	29	38
Biggs EXP6	6	13	18	17	24	23	33	15	34	15	34	21	31
Chebyquad	6	11	17	10	17	11	17	10	17	10	17	11	17
Penalty II	10	29	30	29	30	29	30	29	30	29	30	29	30
Average		13.631	29.11	13.89	29.95	14.16	29.89	13.68	31.11	13.79	31.47	13.84	30.26

Table 2. Numerical results with the BFGS direction

Problem name	Dimension	NMLS-G		NMLS-H		NMLS-N		NMLS-M		NMLS-1		NMLS-2	
		N_i	N_f										
Beale	2	17	24	17	24	24	24	17	24	16	24	17	24
Brown badly scaled	2	18	60	14	57	43	68	48	72	48	72	48	72
Powell badly scaled	2	63	91	63	91	63	88	69	95	63	88	65	90
Variably Dim	2	5	13	5	13	5	13	5	13	5	13	5	13
Watson	2	9	21	9	21	9	21	9	21	9	21	9	21
Box three-dim	3	30	39	30	39	30	39	30	39	30	39	30	39
Gaussian	3	3	6	3	6	3	6	3	6	3	6	3	6
Gulf r. and d.	3	30	40	33	44	30	40	33	44	33	44	33	44
Helical valley	3	50	80	43	73	50	80	38	68	33	60	31	53
Bro. a. Dennis	4	26	80	24	79	26	80	24	79	24	79	24	79
E. Rosenbrock	4	73	89	72	94	73	89	62	85	56	85	70	96
E. Powell singular	4	31	51	36	57	31	51	36	57	24	47	36	57
Penalty I	4	1258	1356	659	659	462	522	479	552	482	546	482	546
Penalty II	4	14	21	14	21	14	21	14	21	12	20	14	21
Trigonometric	4	14	15	13	15	14	15	13	15	13	15	13	15
Wood	4	33	68	30	65	33	68	33	68	30	65	33	68
Biggs EXP6	6	45	58	39	47	45	58	43	58	43	58	45	60
Chebyquad	6	19	32	19	32	19	32	18	32	19	32	18	33
Penalty II	10	1492	1682	1412	1727	509	786	524	781	514	767	648	982
Average		248.46	294.31	186.08	243.38	114.08	161.62	115.23	163.85	112.08	160.08	124.92	173.38

Table 3. Numerical results with the LBFGS direction

Table 3. Numerical results (*continued*)

Table 4. Numerical results with the Barzilai-Borwein direction (BB1)

Problem name	Dimension	NMLS-G		NMLS-H		NMLS-N		NMLS-M		NMLS-1		NMLS-2	
		N_i	N_f	N_i	N_f	N_i	N_f	N_i	N_f	N_i	N_f	N_i	N_f
Beale	2	46	52	42	50	46	53	36	52	38	54	37	54
Brown badly scaled	2	Failed	Failed	8	109	8	109	8	109	8	109	8	109
Full Hess . FH1	2	49	56	43	46	50	75	40	57	42	52	41	53
Full Hess . FH2	2	9	10	9	10	9	10	9	10	9	10	9	10
Gaussian	3	4	14	4	14	4	14	4	14	4	14	4	14
Box three-dim	3	36	62	36	64	36	67	105	219	882	1854	882	1854
Gulf r . and d.	3	1679	4232	2027	5724	4697	16171	43749	118335	36528	99453	2276	6860
Staircase 1	4	13	14	13	14	13	14	13	14	13	14	13	14
Staircase 2	4	13	14	13	14	13	14	13	14	13	14	13	14
Bro . a . Dennis	4	52	56	57	68	52	56	49	62	67	49	62	62
wood	4	242	326	138	154	255	520	1055	2291	222	450	805	1705
Biggs EXP66	6	567	904	1025	1826	4003	9631	3559	7571	3517	7309	4058	8836
Penalty II	10	579	1271	674	1518	2756	7686	1792	4497	1623	3997	1165	2954
Variably Dim	10	1	2	1	2	1	2	1	2	1	2	1	2
E . Powell Sin	16	214	348	145	213	5097	11888	1820	3812	2711	5493	2575	5284
ARGLINB	100	1075	41863	31	592	31	592	31	592	31	592	31	592
Diagonal 3	100	102	119	107	109	106	147	105	150	113	166	103	145
E . Rosenbrock	100	96	208	44	79	63	131	36	82	33	67	36	82
Diagonal 2	500	108	132	111	131	99	156	112	181	130	216	109	177
DIXON3DQ	1000	31289	52569	36487	66657	27809	65253	40299	86697	37983	80702	37983	80702
E . Beal	1000	48	55	41	49	48	55	36	56	35	45	36	55
Fletcher	1000	26718	44020	28940	51865	32507	74158	40440	85575	14475	29456	35721	74592
G . Rosenbrock	1000	24999	38314	24573	41178	23971	40964	25895	50162	25741	49242	26089	50267
Par . Pert . Quadratic	1000	203	270	179	180	305	590	325	592	411	711	433	731
Hager	1000	61	66	57	59	54	65	55	60	57	59	57	59
BDQRTIC	1000	82	91	86	87	80	94	81	106	87	98	69	74
BG2	1000	44	58	99	159	65	88	196	433	57	104	209	464
Purt . Trid . Quadratic	5000	2092	3344	854	1382	1633	3121	1685	3404	1765	3558	1727	3536
Al . Pert . Quadratic	5000	1602	2522	1831	3170	1026	1866	1956	3999	2052	4097	1117	2192
Pert . Quadratic diag	5000	362	595	470	797	1439	4045	1285	3160	1231	2900	977	2330
E . Trid . 1	5000	32	37	32	33	36	47	35	50	31	33	34	42
NONSCOMP	5000	62	63	62	63	54	56	54	57	63	65	54	57
LIARWHD	5000	50	80	45	101	63	122	66	191	40	87	53	139
TRIDIA	5000	8165	13522	11603	21006	10306	21041	14720	31087	17699	37371	14839	31400
DIXMAANA	9000	9	10	9	10	9	10	9	10	9	10	9	10
DIXMAANB	9000	8	9	8	9	8	9	8	9	8	9	8	9
DIXMAANC	9000	10	11	10	11	10	11	10	11	10	11	10	11
DIXMAAND	9000	13	14	13	14	13	14	13	14	13	14	13	14
DIXMAANE	9000	1177	1807	987	1695	821	1831	1061	2176	1039	2081	1023	1986
DIXMAANF	9000	442	675	715	1191	666	1449	641	1335	895	1800	1051	2076
DIXMAANG	9000	1024	1602	835	1377	734	1612	461	903	1022	2031	732	1457

Table 4. Numerical results (*continued*)

	9000	658	1030	924	1528	776	1706	754	1522	966	1929	878	1726
DIXMAANH	9000	6918	11583	6719	12096	6289	14861	10180	2178	7951	16803	9165	19375
DIXMAANM	9000	580	857	475	725	819	1706	661	1239	896	1685	575	1080
DIXMAANK	9000	483	741	636	1020	618	1250	853	1703	596	1087	841	1604
DIXMAANL	9000	379	552	437	644	607	1244	660	1209	629	1176	477	890
ARWHEAD	10000	3	4	3	4	3	4	3	4	3	4	3	4
BDEXP	10000	18	19	18	19	18	19	18	19	18	19	18	19
Broyden Tridiagonal	10000	78	83	71	72	83	98	78	100	72	78	75	96
COSIN	10000	Failed	Failed	33	40	Failed	Failed	33	40	33	40	Failed	Failed
Diagonal 4	10000	3	4	3	4	3	4	3	4	3	4	3	4
Diagonal 5	10000	4	5	4	5	4	5	4	5	4	5	4	5
Ext . Tridiagonal 2	10000	31	36	31	36	30	36	31	36	31	36	31	36
Diagonal 7	10000	7	8	7	8	7	8	7	8	7	8	7	8
Diagonal 8	10000	6	8	6	8	6	8	6	8	6	8	6	8
DQDRATIC	10000	27	28	27	28	27	28	27	28	27	28	27	28
ENGVAL1	10000	28	29	28	29	28	29	28	29	28	29	28	29
EDENSCH	10000	27	28	27	28	27	28	27	28	27	28	27	28
Ext . BDI	10000	16	19	16	19	16	19	16	19	16	20	16	19
Ext . DEN SCHNB	10000	10	11	10	11	10	11	10	11	10	11	10	11
Ext . DEN SCHNF	10000	12	13	12	13	12	13	12	13	12	13	12	13
Ext . Himmelblau	10000	15	18	15	18	15	18	15	18	15	18	15	18
Ext . Maratos	10000	76	127	64	124	101	209	78	202	129	340	85	217
Ext . Powell	10000	360	674	231	397	14866	35239	6512	13509	6920	14447	4413	9095
Ext . Penalty	10000	123	2858	6	67	6	67	6	67	6	67	6	67
Ext . PSC1	10000	17	18	17	18	17	18	17	18	17	18	17	18
Ext . QP1	10000	13	14	13	14	13	14	13	14	10	14	13	14
Ext . QP2	10000	51	106	35	73	26	54	23	47	15	30	25	48
Ext . TET	10000	10	13	10	13	10	13	10	13	10	13	10	13
Ext . Wood	10000	274	365	139	155	281	575	1157	2464	242	464	1163	2474
Ext . White a . Holst	10000	122	157	76	116	103	168	68	154	66	141	68	154
Ext . Tridiagonal 1	10000	32	37	35	37	36	47	36	51	31	33	34	42
FH3	10000	3	4	3	4	3	4	3	4	3	4	3	4
G . PSC1	10000	26	27	26	27	26	27	26	27	26	27	26	27
G . Tridiagonal	10000	26	27	26	27	26	27	26	27	26	27	26	27
HIMMELBG	10000	20	21	20	21	20	21	20	21	20	21	20	21
NONDQUAR	10000	5734	9701	6121	11539	10738	25859	8646	18582	8990	21268	9310	19820
Perturbed	10000	3332	5371	1996	3418	3028	6319	3610	7646	2894	5941	3096	6337
QUARTC	10000	1	2	1	2	1	2	1	2	1	2	1	2
QF1	10000	1914	3035	3367	6017	3070	6296	3901	8223	3339	6896	2887	5878
QF2	10000	1853	3020	1857	3161	2424	4866	2269	4724	2398	4889	3277	6715
Raydan	10000	1	2	1	2	1	2	1	2	1	2	1	2
SINCOS	10000	17	18	17	18	17	18	17	18	17	18	17	18
TRIDIA	10000	21252	35581	28315	51638	18599	38133	24617	52700	25154	53422	30126	64210
Average		2951.65	27514.52	1956.45	3512.77	2759.61	9558.57	2932.75	6493.89	2538.79	5542.02	2991.69	6378.95

Table 5. Numerical results with the Barzilai-Borwein direction (BB2)

Problem name	Dimension	NMLS-G		NMLS-H		NMLS-N		NMLS-M		NMLS-1		NMLS-2	
		N_i	N_f	N_i	N_f	N_i	N_f	N_i	N_f	N_i	N_f	N_i	N_f
Beale	2	30	31	30	31	30	31	31	30	30	35	32	37
Brown badly scaled	2	Failed	Failed	8	109	8	109	8	109	8	109	8	109
Full Hess . FH1	2	38	40	38	40	33	40	38	41	38	44	33	40
Full Hess . FH2	2	9	10	9	10	9	10	9	10	9	10	9	10
Gaussian	3	4	14	4	14	4	14	4	14	4	14	4	14
Box three-dim	3	72	91	75	89	71	93	72	91	71	72	91	91
Gulf r . and d.	3	532	578	762	848	531	633	645	737	690	800	631	742
Staircase 1	4	7	8	7	8	7	8	7	8	7	8	7	8
Staircase 2	4	7	8	7	8	7	8	7	8	7	8	7	8
Bro . a . Dennis wood	4	49	50	49	50	49	50	49	50	49	50	47	51
Biggs EXP66	6	453	495	413	457	605	702	590	661	536	597	473	529
Penalty II	10	223	301	73	76	329	446	433	556	333	436	421	536
Variably Dim	10	1	2	1	2	1	2	1	2	1	2	1	2
E . Powell Sin	16	133	152	120	131	162	220	134	175	140	184	156	205
Watson	31	4961	5148	7062	7312	5216	5606	6798	7100	7677	8102	6079	6472
HARKERP2	50	27851	28183	Failed	Failed	15438	18678	32888	33460	34703	36001	23470	24294
ARGLINB	100	1069	40515	30	591	30	591	30	591	30	591	30	591
Diagonal 3	100	92	93	92	93	108	114	116	121	116	121	116	121
E . Rosenbrock	100	58	65	58	65	64	73	78	73	100	74	102	102
Diagonal 2	500	112	115	103	105	134	145	92	101	115	120	104	120
DIXON3DQ	1000	8286	8363	9367	9488	10934	11188	6567	6654	6856	6958	6567	6654
E . Beal	1000	28	29	28	29	28	29	28	32	28	32	30	36
Fletcher	1000	4569	5626	8089	9784	4445	5550	11476	13223	11407	13141	11385	13112
G . Rosenbrock	1000	24950	28069	23700	26822	23814	26380	23673	26804	25645	28796	23797	26941
Par . Pert . Quadratic	1000	218	233	212	217	244	269	308	328	314	342	314	342
Hager	1000	48	50	48	50	48	50	48	50	48	50	48	50
BDQRTIC	1000	88	89	88	89	93	98	96	100	82	88	82	88
BG2	1000	55	60	55	60	79	99	68	78	75	99	100	118
POWER	1000	29416	29678	14753	14914	27012	27355	28046	28376	25356	25678	21596	21839
Pert . Trid . Quadratic	5000	981	1009	825	852	932	1002	1021	1059	1318	1381	817	817
Al . Pert . Quadratic	5000	840	866	1136	1173	1019	1095	954	1009	935	991	954	1009
Pert . Quadratic diag	5000	273	299	308	312	357	430	299	332	308	353	332	368
E . Hiebert	5000	3181	3185	3181	3185	3181	3185	3181	3185	3181	3185	3181	3185
Fletcher	5000	23321	28385	22936	31043	Failed	Failed	17180	25290	18139	26278	17864	25970
E . Trid . 1	5000	31	32	31	32	31	32	31	32	31	32	31	32
NONSCOMP	5000	47	48	47	48	47	48	47	48	47	48	47	48
LIARWHD	5000	54	55	49	53	49	51	55	71	44	57	47	64
TRIDIA	5000	4804	4913	4076	4162	3574	3685	4319	4409	5477	5634	3334	3430
DIXMAANA	9000	9	10	9	10	9	10	9	10	9	10	9	10
DIXMAANB	9000	8	9	8	9	8	9	8	9	8	9	8	9
DIXMAANC	9000	10	11	10	11	10	11	10	11	10	11	10	11
DIXMAAND	9000	13	14	13	14	13	14	13	14	13	14	13	14
DIXMAANE	9000	537	551	622	647	483	537	853	764	792	809	848	848

Table 4. Numerical results (*continued*)

DIXMAANF	9000	631	637	478	502	473	509	473	489	521	543	312	328
DIXMAANG	9000	527	543	374	382	589	638	595	612	337	361	337	361
DIXMAANH	9000	564	585	678	693	419	453	594	609	500	520	522	550
DIXMAANH	9000	2608	2650	3197	3239	3815	3965	3450	3522	2898	2979	3152	3226
DIXMAANJ	9000	531	546	605	622	634	667	394	404	394	415	406	417
DIXMAANK	9000	364	374	416	428	410	438	395	410	369	389	510	527
DIXMAANL	9000	365	377	435	452	396	424	379	399	324	348	400	420
ARWHEAD	10000	3	4	3	4	3	4	3	4	3	4	3	4
BDEXP	10000	18	19	18	19	18	19	18	19	18	19	18	19
Broyden Tridiagonal	10000	92	95	99	100	97	103	98	109	110	116	97	110
COSIN	10000	Failed	Failed	35	44	Failed	Failed	40	50	35	44	40	65
Diagonal 4	10000	3	4	3	4	3	4	3	4	3	4	3	4
Diagonal 5	10000	4	5	4	5	4	5	4	5	4	5	4	5
Ext . Tridiagonal 2	10000	33	38	33	38	37	44	33	38	33	38	33	38
Diagonal 7	10000	7	8	7	8	7	8	7	8	7	8	7	8
Diagonal 8	10000	6	8	6	8	6	8	6	8	6	8	6	8
DQDRTIC	10000	21	22	21	22	21	22	21	22	21	22	21	22
ENGVAL1	10000	31	32	31	32	31	32	31	32	31	32	31	32
EDENSCH	10000	30	31	30	31	30	31	30	31	30	31	30	31
Ext . BD1	10000	15	18	15	18	15	18	15	18	14	18	15	18
Ext . DEN SCHNB	10000	10	11	10	11	10	11	10	11	10	11	10	11
Ext . DEN SCHNF	10000	13	14	13	14	13	14	13	14	13	14	13	14
Ext . Himmelblau	10000	15	17	15	17	15	17	15	17	15	17	15	17
Ext . Maratos	10000	119	144	115	141	119	144	136	182	135	185	136	182
Ext . Powell	10000	194	226	166	185	187	241	202	273	186	256	243	318
Ext . Penalty	10000	122	2857	5	66	5	66	5	66	5	66	5	66
Ext . PSC1	10000	14	15	14	15	14	15	14	15	14	15	14	15
Ext . QP1	10000	13	14	13	14	13	14	13	14	13	14	13	14
Ext . QP2	10000	51	106	35	73	26	54	23	47	15	30	23	47
Ext . TET	10000	9	12	9	12	9	12	9	12	9	12	9	12
Ext . Wood	10000	607	726	695	804	551	658	691	866	662	845	825	1047
Ext . White a . Hoist	10000	66	68	71	72	66	68	88	107	72	89	88	108
Ext . Tridiagonal 1	10000	33	35	34	35	33	37	33	35	33	37	33	37
FH3	10000	3	4	3	4	3	4	3	4	3	4	3	4
G . PSC1	10000	26	27	26	27	26	27	26	27	26	27	26	27
G . Tridiagonal	10000	24	25	24	25	24	25	24	25	24	25	24	25
HIMMELBG	10000	21	22	21	22	21	22	21	22	21	22	21	22
NONDQUAR	10000	2856	2916	2976	3035	3025	3193	2986	3068	2888	2999	2996	3092
Perturbed	10000	1599	1650	1298	1337	1612	1732	1480	1525	2074	2156	1462	1524
QUARTC	10000	1	2	1	2	1	2	1	2	1	2	1	2
QF1	10000	1043	1097	1909	1961	1636	1714	1259	1313	1854	1925	1282	1339
QF2	10000	1525	1576	1738	1786	1482	1557	1388	1449	1326	1402	1260	1321
Raydan	10000	1	2	1	2	1	2	1	2	1	2	1	2
SINCOS	10000	14	15	14	15	14	15	14	15	14	15	14	15
TRIDIA	10000	9767	9898	5519	5625	5839	5976	5073	5157	5742	5893	10527	10712
Average		2944.38	24306.72	1915.18	2100.42	2489.36	2655.27	1899.83	1998.06	1866.80	2068.75	1672.60	1867.37

References

1. Ahookhosh, M.: Optimal subgradient algorithms with application to large-scale linear inverse problems, submitted, http://www.optimization-online.org/DB_HTML/2014/02/4234.html, (2014) [19]
2. Ahookhosh, M., Amini, K.: An efficient nonmonotone trust-region method for unconstrained optimization. *Numerical Algorithms*, **59**(4), 523–540 (2012) [5]
3. Ahookhosh, M., Amini, K., Bahrami, S.: Two derivative-free projection approaches for systems of large-scale nonlinear monotone equations *Numerical Algorithms*, **64**, 21–42 (2013) [8, 9]
4. Ahookhosh, M., Amini, K., Bahrami, S.: A class of nonmonotone Armijo-type line search method for unconstrained optimization, *Optimization*, **61**(4), 387–404 (2012) [4, 6, 8]
5. Ahookhosh, M., Amini, K., Peyghami, M.R.: A nonmonotone trust-region line search method for large-scale unconstrained optimization, *Applied Mathematical Modelling*, **36**(1), 478–487 (2012) [5]
6. Amini, K., Ahookhosh, M., Nosratipour, H.: An inexact line search approach using modified nonmonotone strategy for unconstrained optimization, *Numerical Algorithms*, **66**, 49–78 (2014) [4, 6, 8, 9]
7. Andretta, M., Birgin, E.G., Martínez, J.M.: Partial spectral projected gradient method with active-set strategy for linearly constrained optimization, *Numerical Algorithms*, **53**, 23–52 (2010) [14]
8. Andrei, N.: An unconstrained optimization test functions collection, *Advanced Modelling and Optimization*, **10**(1), 147–161 (2008) [9]
9. Armijo, L.: Minimization of functions having Lipschitz continuous first partial derivatives, *Pacific Journal of Mathematics*, **16**, 1–3 (1966) [2]
10. Barzilai, J., Borwein, J.M.: Two point step size gradient method, *IMA Journal of Numerical Analysis*, **8**, 141–148 (1988) [14]
11. Bertero, M., Boccacci, P.: *Introduction to Inverse Problems in Imaging*, Bristol, U.K.: IOP, (1998) [19]
12. Birgin, E.G., Martínez, J.M., Raydan, M.: Nonmonotone spectral projected gradient methods on convex sets, *SIAM Journal on Optimization*, **10**, 1196–1211 (2000) [14]
13. Birgin, E.G., Martínez, J.M., Raydan, M.: Inexact spectral projected gradient methods on convex sets, *IMA Journal of Numerical Analysis*, **23**, 539–559 (2003) [14]
14. Bonnans J.F., Panier E., Tits A., Zhou J.L.: Avoiding the Maratos effect by means of a nonmonotone line search, II: Inequality constrained problems – feasible iterates, *SIAM Journal on Numerical Analysis*, **29**, 1187–1202 (1992) [4]
15. Borsdorf, R., Higham, N.J.: A preconditioned Newton algorithm for the nearest correlation matrix, *IMA Journal of Numerical Analysis*, **94**, 94–107 (2010) [2]
16. Cartis, C., Sampaio, Ph.R., Toint, Ph.L.: Worst-case evaluation complexity of non-monotone gradient-related algorithms for unconstrained optimization, *Optimization*, (2014) [4]
17. Chamberlain, R.M., Powell, M.J.D., Lemarechal, C., Pedersen, H.C.: The watchdog technique for forcing convergence in algorithm for constrained optimization, *Mathematical Programming Studies*, **16**, 1–17 (1982) [4]
18. Chambolle, A., Caselles, V., Cremers, D., Novaga, M., Pock, T.: An introduction to total variation for image analysis. In: *Theoretical Foundations and Numerical Methods for Sparse Recovery*, vol. 9, pp. 263340. De Gruyter, Radon Series Comp. Appl. Math. (2010) [19]
19. Dai, Y.H.: On the nonmonotone line search, *Journal of Optimization Theory and Applications*, **112**(2), 315–330 (2002) [4]
20. Dai, Y.H., Fletcher, R.: Projected barzilai-borwein methods for large-scale box-constrained quadratic programming, *Numerische Mathematik*, **100**, 21–47 (2005) [14]
21. Dai, Y.H., Hager, W.W., Schittkowski, K., Zhang, H.: The cyclic Barzilai-Borwein method for unconstrained optimization, *IMA Journal of Numerical Analysis*, **26**, 604–627 (2006) [14]
22. Dai, Y.H., Yuan, J.Y., Yuan, Y.Y.: Modified two-point stepsize gradient methods for unconstrained optimization, *Computational Optimization and Applications*, **22**, 103–109 (2002) [14]
23. Dolan, E., Moré, J.J.: Benchmarking optimization software with performance profiles, *Mathematical Programming*, **91**, 201–213 (2002) [9]
24. R. Fletcher, *Practical methods of optimization*, 2nd Edition, Wiley, 2000, New York [1, 2, 8]
25. Grippo, L., Lampariello, F., Lucidi, S.: A nonmonotone line search technique for Newton's method, *SIAM Journal on Numerical Analysis*, **23**, 707–716 (1986) [2, 4, 8, 9]
26. Grippo, L., Lampariello, F., Lucidi, S.: A truncated Newton method with nonmonotone line search for unconstrained optimization, *Journal of Optimization Theory and Applications*, **60**(3), 401–419 (1989) [4]
27. Grippo, L., Lampariello, F., Lucidi, S.: A class of nonmonotone stabilization methods in unconstrained optimization, *Numerische Mathematik*, **59**, 779–805 (1991) [4]
28. Hager, W.W., Mair, B.A., Zhang, H.: An affine-scaling interior-point CBB method for box-constrained optimization, *Mathematical Programming*, **119**, 1–32 (2009) [14]
29. Judice, J., Raydan, M., Rosa, S., Santos, S.: On the solution of the symmetric eigenvalue complementarity problem by the spectral projected gradient algorithm, *Numerical Algorithms*, **47**, 391–407 (2008) [14]
30. Liu, D.C., Nocedal, J.: On the limited memory BFGS method for large scale optimization, *Mathematical Programming*, **45**, 503–528 (1989) [10]
31. Luengo, F., Raydan, M., Glunt, W., Hayden T.L.: Preconditioned spectral gradient method, *Numerical Algorithms*, **30**, 241–258 (2002) [14]
32. J. Mo, C. Liu, S. Yan, A nonmonotone trust region method based on nonincreasing technique of weighted average of the successive function value, *Journal of Computational and Applied Mathematics* 209 (2007) 97–108. [4]
33. Moré, J.J., Garbow, B.S., Hillstrom, K.E.: Testing unconstrained optimization software, *ACM Transformations on Mathematical Software*, **7**(1), 17–41 (1981) [9, 10]
34. Morini, B., Porcelli, M., Chan, R.H.: A reduced Newton method for constrained linear least-squares problems, *Journal of Computational and Applied Mathematics*, **233**, 2200–2212 (2010) [19, 21]
35. Nesterov, Y.: *Introductory lectures on convex optimization: A basic course*, Kluwer, Dordrecht (2004) [1, 2]
36. Neumaier, A.: Solving ill-conditioned and singular linear systems: A tutorial on regularization, *SIAM Review*, **40**(3), 636–666 (1998) [19]

37. Ng, M., Chan, R., Tang, W.: A fast algorithm for deblurring models with Neumann boundary conditions, *SIAM Journal on Scientific Computing*, **21**, 851–866 (2000) [19]
38. Nocedal, J., Wright, J.S.: *Numerical Optimization*, Second ed., Springer, New York, (2006) [1, 2, 7]
39. Nocedal, J.: Updating quasi-Newton matrices with limited storage, *Mathematics of Computation*, **35**, 773–782 (1980) [10]
40. Ortega, J.M., Rheinboldt, W.C.: *Iterative solution of nonlinear equations in several variables*, Academic Press, New York (1970) [3]
41. Panier, E.R., Tits, A.L.: Avoiding the Maratos effect by means of a nonmonotone linesearch I, *SIAM Journal on Numerical Analysis*, **28**, 1183–1195 (1991) [4]
42. Raydan, M.: The Barzilai and Borwein gradient method for the large scale unconstrained minimization problem, *SIAM Journal on Optimization*, **7**, 26–33 (1997) [14]
43. Toint, Ph.L.: An assessment of nonmonotone linesearch technique for unconstrained optimization, *SIAM Journal on Scientific Computing*, **17**, 725–739 (1996) [2, 4]
44. <http://www.ece.northwestern.edu/~nocedal/software.html> [10]
45. Zhang, H.C., Hager, W.W.: A nonmonotone line search technique and its application to unconstrained optimization, *SIAM Journal on Optimization*, **14**(4), 1043–1056 (2004) [4, 6, 8, 9]